Chronoscalar Ordering, Axial Pseudoscalars, and Anisotropic Transport from Geology to Colliders

Calvin A. Grant
Chronoscalar Dynamics

Abstract

We introduce Chronoscalar Field Theory (CFT), a framework in which time is treated as a physically asymmetric scalar ordering field $T(x)$ whose gradient defines admissible causal structure . In contrast to metric-based cosmologies [**?** **?**], ordering is taken as primary and spacetime geometry as emergent. Hessian-regulated curvature of T induces anisotropic transport and parity-odd torsional responses quantified by an axial pseudoscalar χ, constructed purely from ordering geometry [**?**]. We show that χ can be operationally extracted from macroscopic geological datasets via rose-diagram asymmetries [**?**], projected onto ensemble-averaged observables in high-energy collider experiments [**?** **?**], and related to large-scale cosmological anisotropies [**?**], without introducing new interactions or violating local Lorentz or gauge structure . Within this framework, the beginning of time is reformulated as an initial ordering boundary condition rather than a metric singularity , and the Hubble tension is reinterpreted as a projection effect arising from orientation-dependent sampling of ∇T [**?** **?**]. The theory predicts scale-independent manifestations of axial transport bias across geophysics, collider physics, and cosmology, all belonging to the same mathematical class of pseudoscalar invariants.

Keywords: chronoscalar field theory; time asymmetry; axial pseudoscalar; anisotropic transport; elliptic flow; geological torsion; cosmology

1 Introduction

The physical status of time remains unsettled in fundamental theory. In standard formulations, time enters either as a coordinate parameter in relativistic geometry or as an external ordering variable in quantum dynamics, but is not itself endowed with dynamical structure. Cosmological models consequently attribute the origin of temporal asymmetry to special initial conditions or to entropy growth within an otherwise time-symmetric framework. At the same time, persistent anisotropies are observed across widely separated physical regimes, including geological lineament orientations, astrophysical jet alignments, collider flow harmonics, and low-multipole cosmological correlations. These phenomena are typically treated as system-specific effects, modeled independently using tectonic stress fields, hydrodynamic response, or statistical variance, without a unifying geometric principle.

Chronoscalar Field Theory (CFT) addresses this gap by elevating time to a scalar ordering field $T(x)$ whose gradient $\nabla_\mu T$ defines a preferred direction of admissible ordering. The existence of a nonvanishing ∇T breaks time-reversal symmetry at the level of physical admissibility while preserving local covariance and gauge structure. In this framework, spacetime volume elements are interpreted as emergent level sets of T, and irreversible processes arise from Hessian-regulated curvature of the ordering field rather than from stochastic assumptions. Transport parallel to ∇T remains free, while transverse transport incurs ordering cost, producing anisotropic response and finite-support outcome formation during interactions.

A central object in CFT is the axial pseudoscalar χ, constructed from the oriented transverse Hessian of T. χ quantifies parity-odd torsional transport bias and vanishes identically for mirror-symmetric or isotropic configurations. Importantly, χ is dimensionless and scale-free, allowing its construction from macroscopic path integrals, microscopic ensemble averages, or harmonic decompositions, provided a persistent orientational reference exists. This enables direct comparison between geological statistics, collider observables such as elliptic flow coefficients, and cosmological anisotropy measures, without asserting mechanistic identity between systems.

Within this perspective, the beginning of time is reformulated as an initial ordering boundary condition on T rather than a spacetime singularity. The apparent expansion of the universe reflects the progressive unfolding of admissible ordering surfaces, while discrepancies between early- and late-Universe determinations of the Hubble constant arise from orientation-dependent projection of ∇T onto observational frames. Geological structures exhibiting vertical or torsional dominance, particularly in the Dead Sea–Aegean region, are interpreted as long-lived, low-frequency projections of the same ordering field rather than as isolated tectonic anomalies.

The aim of this work is not to introduce new forces or modify established local dynamics, but to identify a common geometric invariant underlying anisotropic transport across scales. We first formalize the chronoscalar

ordering field and its associated axial pseudoscalar, then present a statistically robust extraction of χ from geological datasets. We subsequently map collider elliptic flow systematics onto the same pseudoscalar class under conservative assumptions, and finally discuss cosmological implications, including a geometric reinterpretation of the Hubble tension. Throughout, emphasis is placed on operational definitions, null-tested statistics, and preservation of standard physical limits.

2 Chronoscalar Lagrangian and Field Equations

We construct a minimal covariant action in which temporal ordering is dynamical and anisotropic transport arises geometrically. The fundamental field is a scalar ordering field $T(x)$ defined on a four-dimensional manifold $(\mathcal{M}, g_{\mu\nu})$ with Levi–Civita connection ∇_μ. Define the scalar invariant

$$X \;\equiv\; g^{\mu\nu}\nabla_\mu T \nabla_\nu T, \tag{1}$$

and, wherever $X \neq 0$, the normalized ordering direction

$$n_\mu \;\equiv\; \frac{\nabla_\mu T}{\sqrt{|X|}}, \qquad n_\mu n^\mu = \mathrm{sgn}(X). \tag{2}$$

The existence of n_μ defines a preferred ordering direction while preserving general covariance.

To separate longitudinal and transverse transport relative to n_μ, introduce the projector

$$P_{\mu\nu} \;\equiv\; g_{\mu\nu} - \mathrm{sgn}(X)\, n_\mu n_\nu, \qquad P_{\mu\nu}n^\nu = 0. \tag{3}$$

Curvature of the ordering field is encoded in the Hessian

$$H_{\mu\nu} \;\equiv\; \nabla_\mu \nabla_\nu T. \tag{4}$$

The chronoscalar action is taken to be

$$S_T \;=\; \int \mathrm{d}^4x\,\sqrt{-g}\,\Big[-\Lambda_T + \frac{M_T^2}{2}\,F(X) - \frac{\beta}{2}\,P^{\mu\alpha}P^{\nu\beta}H_{\mu\nu}H_{\alpha\beta}\Big], \tag{5}$$

where $F(X)$ is a dimensionless function chosen to admit a nonzero vacuum expectation $X = X_\star > 0$, Λ_T sets the ordering baseline, and $\beta > 0$ penalizes transverse curvature of T. The Hessian term suppresses arbitrarily sharp transverse gradients and enforces finite-support outcome formation without introducing dissipation by hand.

Parity-odd transport bias arises from oriented transverse curvature of T. Fix a timelike observer field u^μ with $u_\mu u^\mu = -1$ and define the spatial Levi–Civita tensor $\varepsilon_{\mu\nu\rho} \equiv \varepsilon_{\mu\nu\rho\sigma}u^\sigma$. The axial pseudoscalar is defined covariantly as

$$\chi(x) \;\equiv\; \varepsilon^{\mu\nu\rho}\, n_\mu\, P_\nu{}^\alpha P_\rho{}^\beta\, H_{\alpha\beta}. \tag{6}$$

χ is invariant under proper rotations, odd under parity, and vanishes identically for mirror-symmetric transverse ordering.

The electromagnetic sector is introduced without modifying gauge structure. Let A_μ be the gauge potential, $F_{\mu\nu} = \nabla_\mu A_\nu - \nabla_\nu A_\mu$, and $\tilde{F}^{\mu\nu} = \frac{1}{2}\varepsilon^{\mu\nu\alpha\beta}F_{\alpha\beta}$. Anisotropic transport enters through a constitutive tensor depending on n_μ,

$$S_{\mathrm{EM}} \;=\; \int \mathrm{d}^4x\,\sqrt{-g}\,\Big[-\frac{1}{4}\,\kappa^{\mu\nu\alpha\beta}(n)\,F_{\mu\nu}F_{\alpha\beta}\Big], \tag{7}$$

with

$$\kappa^{\mu\nu\alpha\beta}(n) = \kappa_\perp(X)\,P^{\mu[\alpha}P^{\beta]\nu} + \kappa_\parallel(X)\,\mathrm{sgn}(X)\,n^{[\mu}P^{\nu][\alpha}n^{\beta]}. \tag{8}$$

In the limit $\kappa_\perp, \kappa_\parallel \to 1$, standard Maxwell theory is recovered.

Parity-odd coupling between ordering geometry and electromagnetic transport is captured by

$$S_{\mathrm{odd}} \;=\; -\frac{\lambda_\chi}{4}\int \mathrm{d}^4x\,\sqrt{-g}\,\chi(x)\,F_{\mu\nu}\tilde{F}^{\mu\nu}, \tag{9}$$

which is gauge invariant and contributes only when $\nabla_\mu\chi \neq 0$. No additional propagating degrees of freedom are introduced.

The full action is

$$S \;=\; S_T + S_{\mathrm{EM}} + S_{\mathrm{odd}} + S_{\mathrm{m}}[g,\Psi] + \int \mathrm{d}^4x\,\sqrt{-g}\,J^\mu A_\mu, \tag{10}$$

where S_{m} denotes standard matter fields Ψ minimally coupled to $g_{\mu\nu}$.

Variation with respect to A_μ yields the generalized Maxwell equations

$$\nabla_\mu\big(\kappa^{\mu\nu\alpha\beta}(n)\,F_{\alpha\beta}\big) + \lambda_\chi\,(\nabla_\mu\chi)\,\tilde{F}^{\mu\nu} \;=\; J^\nu, \tag{11}$$

together with $\nabla_{[\mu}F_{\nu\rho]} = 0$. Propagation remains luminal and Lorentzian in the weak-coupling regime, while anisotropic and parity-odd transport effects are controlled by gradients of χ.

Variation with respect to T yields the ordering equation of motion

$$M_T^2\,\nabla_\mu(F_X\,\nabla^\mu T) + \beta\,\nabla_\mu\nabla_\nu\big(P^{\mu\alpha}P^{\nu\beta}H_{\alpha\beta}\big) = \mathcal{S}_{\mathrm{EM}} + \mathcal{S}_{\mathrm{odd}}, \tag{12}$$

where $F_X \equiv \partial F/\partial X$ and the source terms arise from the n_μ-dependence of $\kappa^{\mu\nu\alpha\beta}$ and the pseudoscalar coupling $\chi F\tilde{F}$. Equation (**??**) states that electromagnetic activity and irreversible measurement channels back-react on the ordering field, reorganizing corridor structure rather than acting on a passive background.

3 Statistical Extraction of the Axial Pseudoscalar

Operationally, the axial pseudoscalar χ is accessed through directional statistics constructed from ensembles of oriented structures or trajectories . Let $\theta \in [0, \pi)$

denote the azimuthal orientation of an observed element (e.g., fault trace, volcanic lineament, transport direction), measured relative to a fixed reference axis ϕ. For a dataset of N observations $\{\theta_i\}$, define the empirical directional density

$$p(\theta) \;\equiv\; \frac{1}{N}\sum_{i=1}^{N}\delta(\theta-\theta_i), \tag{13}$$

normalized on $[0,\pi)$ to account for axial (head–tail symmetric) data . The axial pseudoscalar estimator is then defined as

$$\hat{\chi} \;\equiv\; \int_0^{\pi} p(\theta)\,\sin\!\big(2(\theta-\phi)\big)\,\mathrm{d}\theta, \tag{14}$$

which is parity-odd under $\theta \mapsto 2\phi-\theta$ and vanishes identically for isotropic or mirror-symmetric distributions .

In practice, directional data are represented by rose diagrams with K bins centered at angles θ_k and associated nonnegative weights w_k, corresponding either to counts or to total traced length within each bin . Defining the normalized bin weights

$$p_k \;\equiv\; \frac{w_k}{\sum_{j=1}^{K} w_j}, \tag{15}$$

the discrete estimator becomes

$$\hat{\chi} \;=\; \sum_{k=1}^{K} p_k\,\sin\!\big(2(\theta_k-\phi)\big). \tag{16}$$

This estimator is dimensionless, scale-free, and invariant under global rotations of the dataset about the reference axis .

To quantify statistical uncertainty, we treat the binned weights as multinomial samples with total weight $W=\sum_k w_k$. A delta-method estimate of the variance is

$$\mathrm{Var}(\hat{\chi}) \;\approx\; \frac{1}{W}\left[\sum_k p_k s_k^2 - \left(\sum_k p_k s_k\right)^2\right], \qquad s_k \equiv \sin\!\big(2(\theta_k-\phi)\big), \tag{17}$$

yielding $\sigma_\chi=\sqrt{\mathrm{Var}(\hat{\chi})}$. This expression is insensitive to overall intensity rescaling and depends only on directional anisotropy .

Significance is assessed using a mirror-symmetry permutation test, which directly targets the null hypothesis $\hat{\chi}=0$. For each realization, each observation θ_i is independently reflected about the reference axis with probability 1/2,

$$\theta_i' = \begin{cases} \theta_i, & u_i < \tfrac{1}{2}, \\ 2\phi-\theta_i \pmod{\pi}, & u_i \ge \tfrac{1}{2}, \end{cases} \qquad u_i \sim \mathrm{Unif}(0,1), \tag{18}$$

and a surrogate $\hat{\chi}^{(b)}$ is computed using Eq. (**??**). Repeating this procedure B times yields an empirical null distribution against which the observed $\hat{\chi}_{\mathrm{obs}}$ is compared. The two-sided permutation p-value is

$$p_{\mathrm{perm}} = \frac{1+\sum_{b=1}^{B}\mathbf{1}\big(|\hat{\chi}^{(b)}| \ge |\hat{\chi}_{\mathrm{obs}}|\big)}{B+1}. \tag{19}$$

Because the permutation acts only on parity, this test is insensitive to binning choice, sample size, and radial weighting, isolating axial torsional bias .

To probe spatial organization, we define a radial pseudoscalar profile $\hat{\chi}(r)$ by partitioning observations into annuli $\mathcal{A}_m=\{i : r_i \in [r_m, r_{m+1})\}$ centered on the reference point . Within each annulus, $\hat{\chi}(r_m)$ is computed via Eq. (**??**). This construction permits identification of distinct morphological regimes. Empirically, the observed structure is consistent with a suppressed near-field core, a torsion-dominated intermediate shell, and decay toward isotropy at large r, which may be parameterized phenomenologically as

$$\hat{\chi}(r) \;\simeq\; A\exp\!\left[-\frac{(r-r_\star)^2}{2\sigma_r^2}\right]\exp\!\left(-\frac{r}{r_d}\right), \tag{20}$$

without asserting a unique functional form .

All reported values of $\hat{\chi}$ are obtained using identical estimators, identical null tests, and control datasets selected to match sampling density and resolution. In particular, near-field regions dominated by vertical or spheroidal structures and far-field control regions (e.g., Greenland, Lake Titicaca) yield $\hat{\chi}\approx 0$ within uncertainty, validating the estimator and permutation framework . The same methodology is applied unchanged in subsequent sections when mapping ensemble-averaged anisotropies in collider observables onto the χ-class of axial pseudoscalars .

4 Collider Projection: CMS/ALICE v_2 Systematics as χ-Class Observables

High-energy nuclear and hadronic collisions provide large ensembles in which weak but persistent azimuthal anisotropies may be measured with high statistical precision . Experimentally, these anisotropies are conventionally characterized by a Fourier decomposition of the final-state azimuthal particle distribution,

$$\frac{\mathrm{d}N}{\mathrm{d}\varphi} \;\propto\; 1+2\sum_{n=1}^{\infty} v_n\cos\!\big(n(\varphi-\Psi_n)\big), \tag{21}$$

where φ is the particle azimuthal angle and Ψ_n denotes the nth-order event-plane orientation . The second harmonic coefficient v_2 (elliptic flow) is of particular interest due to its persistence across collision systems and energies .

In the Chronoscalar Field Theory framework, such observables are not interpreted as evidence for additional interactions, but as ensemble projections of anisotropic

transport relative to the ordering direction $n_\mu \propto \nabla_\mu T$. The relevant classification is geometric rather than dynamical: v_2 is an even-parity harmonic proxy that may encode the presence of an underlying axial, parity-odd transport bias when averaged over large ensembles with a fixed orientational reference .

To place collider observables in the same mathematical class as the axial pseudoscalar defined in Section III, consider the transverse-plane projection of the ordering gradient. Let indices $i, j \in \{x, y\}$ label the plane orthogonal to the beam direction, and let $\hat{p}_j$ denote the unit transverse momentum of a detected particle. Define an event-averaged axial statistic

$$\chi_{\rm coll} \;\equiv\; \left\langle \varepsilon^{ij}\,(\partial_i T)\,\hat{p}_j\,W(p_T,\eta)\right\rangle, \tag{22}$$

where ε^{ij} is the two-dimensional Levi–Civita symbol, p_T is the transverse momentum, η the pseudorapidity, and $W(p_T,\eta)$ an acceptance and phase-space weight encoding experimental cuts and efficiencies . By construction, $\chi_{\rm coll}$ is axial and changes sign under parity in the transverse plane .

The connection to experimentally reported harmonics follows from symmetry considerations. Expanding the single-particle distribution to leading order in a weak ordering gradient and integrating over parity-related contributions yields

$$v_2 \;\sim\; G_{\rm det}\,\chi_{\rm coll}, \tag{23}$$

where $G_{\rm det}$ is a geometry- and detector-dependent proportionality factor that absorbs details of event-plane reconstruction, multiplicity weighting, and kinematic selection . Equation (**??**) asserts only that v_2 and $\chi_{\rm coll}$ occupy the same invariance class as ensemble-averaged measures of anisotropic transport; it does not assert mechanistic identity.

This classification is consistent with several empirical features of collider data. Nonzero v_2 values persist in small collision systems and at low multiplicity, where conventional hydrodynamic assumptions are challenged , suggesting sensitivity to initial-state geometry or ordering rather than to late-time collective flow alone. Within CFT, such persistence reflects the projection of a weak but coherent ordering field onto large statistical ensembles, with finite-support outcome formation occurring during hadronization and detection.

Importantly, the mapping in Eq. (**??**) preserves local Lorentz invariance and gauge structure. In the weak-coupling limit of Section II, propagation remains luminal and standard quantum field theoretic calculations of scattering amplitudes are unchanged . Ordering effects enter only through ensemble-level anisotropies and parity classification, placing collider flow observables, geological torsion statistics, and cosmological anisotropies within a unified geometric framework without introducing new degrees of freedom.

The $\chi_{\rm coll}$ construction in Eq. (**??**) is directly testable. Reweighting v_2 measurements by parity-sensitive observables, pseudorapidity sign, or detector orientation relative to a fixed laboratory frame provides a means of probing axial components of transport bias without altering standard analysis pipelines . Such tests are deferred to future work.

5 Cosmological Projection: Ordering Boundary, Expansion, and Hubble Tension

In Chronoscalar Field Theory, cosmological evolution is governed not by a fundamental scale factor, but by the geometry of the ordering field $T(x)$ and its gradient $n_\mu \propto \nabla_\mu T$. The onset of time is defined as an initial boundary condition on T, characterized by a nonvanishing ordering gradient established over a finite domain,

$$\nabla_\mu T \;\neq\; 0 \quad \text{for } T \geq T_0, \tag{24}$$

where T_0 labels the first admissible ordering surface . No metric singularity is required; the boundary condition fixes orientation and magnitude of admissible temporal ordering rather than initial spacetime curvature.

Spacetime volume elements emerge as level sets of T. Consider a foliation by hypersurfaces $\Sigma_T = \{x : T(x) = \text{const}\}$. The physical three-volume element evolves according to

$$\mathrm{d}V(T) \;\propto\; \sqrt{h}\,\mathrm{d}^3x, \tag{25}$$

where h is the determinant of the induced metric on Σ_T . The effective expansion rate measured by comoving observers with four-velocity u^μ is then

$$H_{\rm eff} \;\equiv\; \frac{1}{3}\nabla_\mu u^\mu \;=\; \frac{1}{3}\,P^{\mu\nu}\nabla_\mu n_\nu \;=\; \frac{1}{3}\,P^{\mu\nu}\frac{H_{\mu\nu}}{\sqrt{|X|}}, \tag{26}$$

where $P_{\mu\nu}$ is the transverse projector defined in Eq. (II.3). Thus, expansion is identified with the transverse divergence of the ordering direction, not with a fundamental metric degree of freedom .

Because $H_{\rm eff}$ depends explicitly on projection onto $P_{\mu\nu}$, it is generically orientation-dependent. Observables sensitive to different angular averages of $\nabla_\mu T$ therefore infer different effective expansion rates . Let $\langle\cdot\rangle_\Omega$ denote averaging over solid angle. Then

$$H_{\rm eff}^{\rm (obs)} \;\equiv\; \left\langle \frac{1}{3}P^{\mu\nu}\nabla_\mu n_\nu \right\rangle_{\Omega_{\rm obs}} \;\neq\; \left\langle \frac{1}{3}P^{\mu\nu}\nabla_\mu n_\nu \right\rangle_{\Omega_{\rm CMB}}, \tag{27}$$

where $\Omega_{\rm obs}$ denotes the angular sampling of a given probe.

Early-Universe observables anchored to the cosmic microwave background effectively sample a nearly global angular average of ∇T, yielding a value $H_0^{\rm CMB}$ close to the isotropic mean . Late-Universe distance ladder measurements, by contrast, probe local or anisotropically

weighted projections of the same ordering field, yielding a value $H_0^{\rm local} = H_0^{\rm CMB} + \Delta H_0$ with

$$\Delta H_0 \;\sim\; \langle P^{\mu\nu}\nabla_\mu n_\nu\rangle_{\rm local} - \langle P^{\mu\nu}\nabla_\mu n_\nu\rangle_{\rm global}\,. \qquad (28)$$

This provides a geometric reinterpretation of the Hubble tension as a projection effect rather than as evidence for multiple expansion histories or additional dark components .

The same ordering field admits parity-odd structure through the axial pseudoscalar χ defined in Eq. (II.7). On cosmological scales, χ reduces to a low-frequency torsional mode of the ordering geometry,

$$\chi_{\rm cosmo} \;\sim\; \varepsilon^{ijk} n_i \partial_j n_k, \qquad (29)$$

which vanishes for perfectly isotropic ordering but survives as a frozen harmonic when transverse curvature is present at early times . Such frozen-in modes naturally generate preferred-axis correlations in low-ℓ multipoles without violating statistical isotropy at high ℓ.

Importantly, the cosmological ordering boundary condition propagates into lower-energy systems as a persistent geometric bias. Geological structures exhibiting vertical dominance or torsional shells, as quantified by the radial profile $\hat{\chi}(r)$ in Section III, are interpreted as static, low-frequency projections of the same global ordering direction . No causal influence from cosmological distances is required; persistence replaces propagation.

In the weak-curvature limit where transverse Hessian terms are negligible and $\chi \to 0$, Eq. (**??**) reduces to the standard isotropic expansion law, and the theory reproduces the phenomenology of ΛCDM at leading order . Deviations enter only through controlled, dimensionless projections of the ordering field, rendering the framework falsifiable through directional dependence of expansion observables and axial statistics.

5.1 Ordering Boundary at $T = 0$

Chronoscalar Field Theory does not admit an ontological instant preceding ordering . The earliest physically meaningful state is defined by the emergence of a nontrivial ordering gradient at a boundary surface $T = 0$. Formally, this boundary is characterized by

$$T(x) = 0, \qquad \nabla_\mu T \neq 0, \qquad (30)$$

with no assumption of pre-existing spacetime geometry . The condition $\nabla_\mu T \neq 0$ selects a preferred ordering direction n_μ and thereby breaks time-reversal symmetry at the level of admissibility rather than dynamics .

At $T = 0$, the metric $g_{\mu\nu}$ is not assumed to satisfy any Friedmann-type constraint . Instead, the ordering field defines a congruence of admissible curves along which physical processes may be sequenced . This constitutes a Machian initialization: global ordering is fixed once, and all subsequent local dynamics are constrained by this boundary condition [**?**]. No local observable depends on absolute values of T, only on its gradient and curvature.

The Machian character follows from the absence of local degrees of freedom capable of reorienting n_μ after initialization . Once selected, the global orientation of $\nabla_\mu T$ persists and acts as a geometric background against which inertia, transport, and causality are defined .

5.2 Asymmetry Selection and Non-Commutation of Limits

The emergence of temporal asymmetry at $T = 0$ is not the result of spontaneous symmetry breaking in a potential landscape, but of a non-commutation between the limits

$$\lim_{T\to 0^+} \nabla_\mu T \qquad \text{and} \qquad \lim_{\epsilon\to 0} \delta T, \qquad (31)$$

where δT denotes fluctuations of the ordering field . Finite-support admissibility requires that outcome formation and transport occur over nonzero ordering intervals, so the limit $\delta T \to 0$ is inadmissible at $T = 0$.

As a result, the initial ordering gradient cannot average to zero, even if the underlying configuration space admits symmetric configurations . This mechanism selects a definite orientation for n_μ without invoking stochastic symmetry breaking or fine-tuning . The resulting asymmetry is global, persistent, and encoded in the sign and orientation of $\nabla_\mu T$.

This non-commutation also fixes the arrow of time. Reversing n_μ would require transport through $T < 0$, which is excluded by construction . Thus, irreversibility is imposed geometrically rather than dynamically, and entropy production appears as a consequence of transverse curvature relative to the fixed ordering direction .

5.3 Carving of Spatial Dimensions from Ordering

Spatial dimensionality emerges as a secondary construct once a global ordering direction is fixed . Given a nonvanishing n_μ, the transverse projector

$$P_{\mu\nu} = g_{\mu\nu} - \mathrm{sgn}(X)\, n_\mu n_\nu \qquad (32)$$

defines a three-dimensional subspace orthogonal to admissible ordering. Physical space is identified with equivalence classes of points on hypersurfaces Σ_T defined by $T = \text{const}$.

The carving of spatial dimensions is therefore instantaneous with respect to ordering, but not with respect to any pre-existing time coordinate . Once n_μ is established, three transverse degrees of freedom are immediately available for transport, curvature, and interaction. No additional compactification or dimensional reduction mechanism is required .

Importantly, the speed of light emerges as a kinematic bound associated with propagation along admissible corridors defined by n_μ . Transverse motion relative to the ordering direction incurs Hessian-regulated cost, while longitudinal propagation remains free. This distinction fixes a universal limiting speed without invoking a medium:

$$c \equiv \text{maximal admissible transverse-to-longitudinal transport ratio,} \tag{33}$$

which is invariant under local boosts preserving n_μ and reduces to the standard Lorentz-invariant bound in the weak-curvature limit [**?**].

In this sense, space is carved by ordering, and causality is inherited from the geometry of T rather than imposed axiomatically .

5.4 Early-Time Torsion and Frozen-In Axial Modes

At early ordering times, transverse curvature of T need not vanish . The axial pseudoscalar

$$\chi = \varepsilon^{\mu\nu\rho}\, n_\mu P_\nu{}^\alpha P_\rho{}^\beta H_{\alpha\beta} \tag{34}$$

therefore admits nonzero low-frequency modes . As ordering progresses and transverse degrees stiffen, these modes freeze, leaving residual parity-odd structure encoded in χ .

On cosmological scales, such frozen-in torsion manifests as preferred-axis correlations in low-ℓ multipoles, while averaging to zero at small scales . On geological scales, the same frozen modes project as vertical spheroidal cores and torsional shells in structural statistics . In collider ensembles, they appear only statistically, through parity-classified anisotropies such as v_2 .

Thus, the Machian event at $T = 0$ seeds a hierarchy of persistent axial structures whose manifestations depend solely on scale and projection, not on separate physical mechanisms [**?**].

5.5 Summary of the $T = 0$ Sequence

The chronoscalar cosmological sequence may be summarized as:

$$\boxed{\begin{array}{c} T = 0 \;\longrightarrow\; \nabla T \neq 0 \;\longrightarrow\; \text{asymmetry} \\ \text{selection} \;\longrightarrow\; \text{spatial carving} \\ \longrightarrow\; \text{persistent axial structure} \end{array}} \tag{35}$$

with no intermediate singularity, no stochastic symmetry breaking, and no modification of local field dynamics . All subsequent physical phenomena inherit their causal ordering, anisotropic transport properties, and irreversibility from this initial Machian boundary condition [**?**].

6 Finite-Support Ordering and the Emergence of Geometric Transport Bounds

Let $\mathcal{M}$ be a smooth differentiable manifold. We assume no metric, no causal structure, and no pre-existing notion of distance or duration [**?**]. The only primitive object is a scalar ordering field

$$T : \mathcal{M} \to \mathbb{R}, \tag{36}$$

which assigns to each point an ordering label. At this stage T is not identified with physical time; it is an ordering coordinate only [**?**].

The foundational admissibility axiom is *finite support* in T: no physical configuration is permitted to have support on a set of measure zero in T . Operationally, every admissible process occupies an interval $\Delta T > 0$. This is not a regularization; it is an ontological restriction. Any attempt to describe a physical configuration "at $T = T_0$" is understood only as a coarse slice of a finite-support structure .

Finite-support admissibility immediately implies that the appropriate mathematical objects are not pointwise states but *ordering-supported bundles* . Consider an admissible trajectory $\gamma : \lambda \mapsto x^\mu(\lambda)$. Define its tangent $v^\mu = dx^\mu/d\lambda$. The ordering advance is

$$\dot{T} \equiv \frac{dT}{d\lambda} = \nabla_\mu T\, v^\mu. \tag{37}$$

Because admissible structures require $\Delta T > 0$, we demand $\dot{T}$ be integrable and non-vanishing on admissible segments:

$$\int_{\lambda_1}^{\lambda_2} \dot{T}\, d\lambda = \Delta T > 0 \qquad \Rightarrow \qquad \dot{T} \not\equiv 0 \quad \text{on admissible segments.} \tag{38}$$

This condition replaces any primitive assumption of "forward time" with a support-based admissibility rule .

The stability of admissible ordering requires second-order structure. We therefore introduce the Hessian of T,

$$H_{\mu\nu} \equiv \nabla_\mu \nabla_\nu T. \tag{39}$$

Because no metric is assumed, $H_{\mu\nu}$ is not a curvature tensor in the Riemannian sense; it is a *stability operator* for ordering support . To see why H is forced, consider a transverse perturbation $x^\mu \to x^\mu + \epsilon\, \xi^\mu$ and expand T along the perturbed curve:

$$T(x+\epsilon\xi) = T(x) + \epsilon\, \nabla_\mu T\, \xi^\mu + \frac{\epsilon^2}{2}\, H_{\mu\nu}\, \xi^\mu \xi^\nu + \mathcal{O}(\epsilon^3). \tag{40}$$

Finite support requires that transverse excursions do not destroy the existence of a finite ΔT ordering interval

. This demands that admissible transverse directions must lie in stability cones defined by H. In particular, directions ξ for which $H_{\mu\nu}\xi^\mu\xi^\nu$ is strongly positive destabilize ordering (small transverse excursions push the ordering label too rapidly, fragmenting finite support), whereas directions with $H_{\mu\nu}\xi^\mu\xi^\nu \le 0$ can remain stable or marginal.

This motivates the definition of *corridors* as sets of directions in the tangent bundle that preserve finite-support stability:

$$\mathcal{C}_p \equiv \Big\{ v^\mu \in T_p\mathcal{M} : \int_{\lambda_1}^{\lambda_2} \dot{T}\, d\lambda > 0 \quad \text{and } H_{\mu\nu}\xi^\mu\xi^\nu \le 0 \quad \text{for admissible transverse } \xi \Big\}. \tag{41}$$

Corridors are therefore not *paths in spacetime* (spacetime is not yet defined); they are *stability bundles* in ordering geometry .

Once corridors exist over extended regions, the theory admits an operational construction of an induced bilinear form. The key is that finite support allows repeatable comparison of transverse and longitudinal stability . Define an admissible family of neighboring trajectories $\gamma_s(\lambda)$ parameterized by s, with separation vector $\xi^\mu = \partial x^\mu/\partial s$. We define an induced quadratic form $g^{\rm ind}_{\mu\nu}$ by the requirement that it reproduce the empirically stable ratio between transverse separation and ordering advance over a finite-support interval. Concretely, for admissible segments,

$$\frac{d}{d\lambda}\left(\xi^\mu \nabla_\mu T\right) = \xi^\mu H_{\mu\nu} v^\nu, \tag{42}$$

and the stability of corridor bundles implies that the growth of transverse separation relative to ordering advance is bounded. We therefore define the induced transverse norm by stipulating that there exists a functional $\|\xi\|_\perp$ such that

$$\|\xi\|_\perp^2 \equiv g^{\rm ind}_{\mu\nu}\,\xi^\mu\xi^\nu \quad \text{with} \quad \frac{d}{d\lambda}\|\xi\|_\perp^2 \text{ bounded on admissible segments.} \tag{43}$$

This step is the point at which *geometry is induced from ordering persistence*, rather than assumed .

With $g^{\rm ind}_{\mu\nu}$ defined, one can form

$$X \equiv g^{{\rm ind}\,\mu\nu}\nabla_\mu T \nabla_\nu T, \tag{44}$$

and, on domains where $X \neq 0$, define the normalized ordering covector

$$n_\mu \equiv \frac{\nabla_\mu T}{\sqrt{|X|}}. \tag{45}$$

This allows the decomposition of tangent directions into longitudinal and transverse components relative to ordering. Define the projector

$$P_{\mu\nu} \equiv g^{\rm ind}_{\mu\nu} - \mathrm{sgn}(X)\, n_\mu n_\nu. \tag{46}$$

The crucial emergent bound is now forced by finite support. Since admissible configurations must occupy $\Delta T > 0$, transverse excursion per unit ordering advance cannot be arbitrarily large. We therefore define the *ordering transport bound* as the supremum over admissible tangents,

$$\kappa \equiv \sup_{v\in\mathcal{C}} \left(\frac{\sqrt{P_{\mu\nu}v^\mu v^\nu}}{|n_\rho v^\rho|} \right), \tag{47}$$

where $\mathcal{C}$ denotes the set of corridor-admissible directions. Equation (**??**) is a definition, but its finiteness is not: $\kappa < \infty$ is a theorem-level consequence of finite-support admissibility . If κ were unbounded, there would exist sequences of admissible motions with arbitrarily large transverse excursion per unit ordering advance, which would fragment ordering support and violate the axiom $\Delta T > 0$.

At this stage κ is not "the speed of light". It is the maximal ratio of transverse-to-longitudinal admissible transport implied by ordering stability. Only after spacetime coordinates are constructed (as labels for stable ordering relations) does κ acquire the operational interpretation of a universal propagation bound. The identification

$$c \equiv \kappa \tag{48}$$

is therefore not postulated but inferred [**?**]. c is the emergent maximal admissible ordering-transport ratio, measured in the induced spacetime bookkeeping system.

The remainder of the theory consists in showing how distinct physical regimes correspond to distinct classes of admissible support relative to this bound: (i) minimal-support transport saturating $P_{\mu\nu}v^\mu v^\nu \to 0$ (radiation), (ii) persistent transverse support $P_{\mu\nu}v^\mu v^\nu > 0$ (mass), and (iii) Hessian-driven selection and reconfiguration of corridor stability (gravity-like phenomena) [**?**]. Importantly, the bound c is already fixed here, before any particle ontology is introduced.

7 Radiation, Mass, and Gravitational Bias as Regimes of Ordering Support

Having constructed the induced decomposition into longitudinal and transverse components relative to ordering, we now define an admissibility action that encodes finite-support cost . The action is not assumed to be a standard spacetime action; it is an ordering-support functional built from the induced objects $(n_\mu, P_{\mu\nu})$ and the stability operator derived from H .

Consider an admissible curve γ with tangent v^μ. Finite-support admissibility requires that transverse engagement produce cost. A minimal general functional consistent

with positivity and reparameterization invariance is

$$\mathcal{A}[\gamma] = \int_\gamma \left(|n_\mu v^\mu| + \alpha \sqrt{P_{\mu\nu} v^\mu v^\nu} + \beta \frac{P_{\mu\nu} v^\mu v^\nu}{|n_\rho v^\rho|} \right) d\lambda, \tag{49}$$

where α, β are nonnegative constants determined by the normalization choices implicit in the construction of $g^{\rm ind}_{\mu\nu}$. The first term measures longitudinal ordering advance (needed to maintain $\Delta T > 0$); the remaining terms measure persistent transverse support. The specific functional form in (**??**) is not arbitrary: (i) the square-root term is the minimal homogeneous degree-one penalty for transverse support, and (ii) the ratio term encodes the empirically forced fact that transverse engagement competes with ordering advance (the same ratio that defines κ) .

We now define physical regimes in terms of variational classes of $\mathcal{A}$.

Radiation as minimal persistent transverse support. A limiting class of admissible curves is defined by

$$P_{\mu\nu} v^\mu v^\nu \to 0, \tag{50}$$

while maintaining $|n \cdot v| > 0$ on admissible segments. Such trajectories minimize the transverse terms in (**??**) and therefore transport ordering with vanishing persistent transverse support. They saturate the admissibility transport bound: in the limit (**??**), the ratio in (**??**) approaches its supremum. In the induced spacetime bookkeeping, this is precisely the propagation at the maximal admissible rate c [**?**].

The essential point is that radiation is not introduced as a field *a priori*. It is the regime of admissible transport in which persistent transverse support collapses to the marginal corridor boundary, $Pvv \to 0$, while the ordering advance remains finite. The wave character of radiation arises because corridor marginality generically implies oscillatory stability: when the projected Hessian eigenvalues $\lambda_i(\mathcal{S})$ approach zero, the system sits at the boundary between convergent and divergent transverse support, producing repeated engagement/disengagement of transverse stability . This is the ordering-level origin of harmonic propagation without assuming a material medium.

Mass as persistent transverse ordering engagement. Massive behavior corresponds to admissible trajectories with

$$P_{\mu\nu} v^\mu v^\nu > 0 \quad \text{over finite-support intervals.} \tag{51}$$

In this class, the transverse terms in (**??**) are nonzero. Define the *persistent transverse support density* along γ,

$$\mu(\lambda) \equiv \sqrt{P_{\mu\nu} v^\mu v^\nu}. \tag{52}$$

The integrated transverse support over an ordering interval,

$$M_T[\gamma] \equiv \int_{\gamma(\Delta T)} \mu(\lambda)\, d\lambda, \tag{53}$$

plays the role of an inertial measure: changing γ changes M_T and therefore changes the ordering cost. Inertia is therefore the variational stiffness of persistent transverse support [**?**]. In CFT language, mass is stabilized ordering engagement, not substance.

Gravity as Hessian selection acting on persistent support. The next step is to derive the gravity-analogue: the bias of massive trajectories toward regions of corridor stability set by $H_{\mu\nu}$. We use the projected Hessian stability operator

$$\mathcal{S}_{\mu\nu} \equiv P_\mu{}^\alpha P_\nu{}^\beta H_{\alpha\beta}. \tag{54}$$

Since $\mathcal{S}$ determines transverse stability, admissibility requires that the ordering action include coupling of transverse support to $\mathcal{S}$. The minimal such coupling adds a term

$$\Delta\mathcal{A}[\gamma] = \int_\gamma \gamma_0 \frac{\mathcal{S}_{\mu\nu} v^\mu v^\nu}{|n_\rho v^\rho|}\, d\lambda, \tag{55}$$

with γ_0 a constant fixed by the relative normalization of T and the induced bilinear form. The ratio structure in (**??**) is forced: $\mathcal{S}_{\mu\nu} v^\mu v^\nu$ measures the stability-weighted transverse engagement, and division by $|n \cdot v|$ enforces finite-support scaling (per unit ordering advance) [**?**].

Varying the full action $\mathcal{A} + \Delta\mathcal{A}$ yields Euler–Lagrange equations that bias trajectories according to gradients of the stability operator. Suppressing algebraic details, the leading-order form of the resulting equation of motion is

$$\frac{Dv^\mu}{d\lambda} = -\,\Gamma^\mu{}_{\alpha\beta} v^\alpha v^\beta - \eta_0\, P^{\mu\alpha}\, \mathcal{S}_{\alpha\beta}\, v^\beta + \cdots, \tag{56}$$

where $\Gamma^\mu{}_{\alpha\beta}$ is the connection compatible with the induced geometry (appearing only after the induced bilinear form exists), η_0 is a constant determined by γ_0 and the normalization conventions, and the ellipsis denotes higher-order terms in transverse engagement and Hessian gradients. Equation (**??**) is the explicit expression of the "Hessian flip" picture: when eigenstructure of $\mathcal{S}$ changes, stable directions open or close, and massive trajectories drift accordingly [**?**].

Why the gravity-update bound equals the radiation bound. We now show why the "speed of gravity" equals the maximal transport bound c *without assuming it.* The key is that gravity in CFT is not a separate interaction carried by an auxiliary field; it is reconfiguration of the same stability operator $\mathcal{S}$ that defines admissibility.

Consider a perturbation δT of the ordering field. The induced change in the Hessian is $\delta H_{\mu\nu} = \nabla_\mu \nabla_\nu (\delta T)$, and

hence the induced change in the stability operator is

$$\delta\mathcal{S}_{\mu\nu} = P_\mu{}^\alpha P_\nu{}^\beta \nabla_\alpha \nabla_\beta (\delta T) \; + \; (\delta P)\cdot H \; + \; P\cdot(\delta g^{\rm ind})\cdot H, \tag{57}$$

where the additional terms reflect that P and $g^{\rm ind}$ themselves depend on T through the induced normalization procedure .

Finite-support admissibility implies that δT cannot be defined instantaneously at a distance: it must occupy finite support in T, and its domain of definition expands only as ordering support expands . Let $\Omega(\Delta T)$ denote the domain reached by the ordering support after ordering interval ΔT has elapsed. Then $\delta\mathcal{S}$ is defined only on $\Omega(\Delta T)$, and cannot be defined on its complement. Therefore any "gravitational change" in (**??**) is not a signal propagating through an existing spacetime but the appearance of a newly-defined $\mathcal{S}$ on an expanding admissibility domain.

But the boundary of $\Omega(\Delta T)$ is exactly the admissibility front whose maximal transverse-to-longitudinal ratio defines κ in (**??**). Thus the expansion of the domain on which $\delta\mathcal{S}$ is defined is bounded by κ, and the induced spacetime bookkeeping identifies

$$\text{maximal admissibility-front speed} = \kappa = c. \tag{58}$$

This is the explicit sense in which gravitational updates "move at c" in CFT: not because gravity is a radiation field, but because both EM transport and Hessian reconfiguration are bounded by the same finite-support ordering front [**?**].

The conclusion is not an analogy but a derived identity: the same admissibility geometry that yields radiation as the minimal-support mode yields the speed limit for stability reconfiguration. The coincidence is therefore structural and non-accidental.

8 Machian Ordering at $T = 0^+$: Corridor Saturation, Asymmetric Projection, and the Origin of Matter Excess

We now analyze the onset of spacetime content immediately following the ordering boundary $T = 0$ [**?**]. The defining feature of this regime is that induced spacetime thermodynamics is not yet established: there is no globally-defined equilibrium temperature, no conserved particle numbers, and no meaningful "reaction rates" in the conventional sense . What exists is ordering support, corridor stability, and finite-support energy stored in that stability.

Define an ordering energy functional associated with corridor stability. Because $H_{\mu\nu}$ (and hence $\mathcal{S}_{\mu\nu}$) governs whether transverse support remains admissible, a natural invariant measure of stored ordering energy is a functional of the stability eigenvalues . Let λ_i denote the eigenvalues of $\mathcal{S}_{ij}$ in a local frame adapted to n_μ. Define the corridor energy density as

$$\rho_{\rm corr} \equiv \mathcal{F}(\{\lambda_i\}; \ell_T)\,, \tag{59}$$

where ℓ_T is the ordering correlation scale and $\mathcal{F}$ is constrained only by: (i) positivity, (ii) increase with increasing stiffness of admissible support, and (iii) reduction to zero at perfect marginality $\lambda_i \to 0$ where no ordering energy is stored. A minimal representative choice (used here for explicitness) is

$$\rho_{\rm corr} = \frac{1}{\ell_T^4} \sum_i \Theta(-\lambda_i)\,|\lambda_i|^\sigma, \qquad \sigma > 0, \tag{60}$$

where Θ enforces that only stabilizing (negative) directions store persistent ordering energy . The precise exponent σ is not essential to the logic; the existence of a saturating energy functional is.

Finite-support admissibility forces saturation. Corridors cannot store arbitrary ordering energy because transverse support must remain finite and stable; beyond a threshold, additional ordering energy cannot be accommodated without changing corridor topology (a Hessian flip) . This is expressed as a bound

$$\rho_{\rm corr} \le \rho_{\max}(\ell_T, \{\lambda_i\}), \tag{61}$$

with $\rho_{\max}$ finite for fixed ℓ_T and bounded eigenstructure. When $\rho_{\rm corr} \to \rho_{\max}$ locally, additional ordering energy cannot remain stored in corridor stability. The only admissible resolution is *projection* into emergent spacetime degrees of freedom: ordering energy overflow becomes spacetime excitation.

This is the precise meaning of "space from ordering" . Spacetime content is not assumed at $T = 0^+$; it is generated by the dynamical necessity of relieving corridor saturation while preserving finite support.

We now show how matter–antimatter asymmetry arises without inserting a CP-violating term in a spacetime Lagrangian. In conventional language, baryogenesis requires a sign-definite asymmetry that survives thermalization . In CFT, the critical observation is that the projection event occurs *before* equilibrium exists; there is no requirement that particle production be symmetric . The symmetry is not broken by an interaction; it is absent because spacetime statistical description is not yet defined.

Projection inherits orientation from ordering geometry. The only oriented object available at $T = 0^+$ is n_μ and the oriented eigenstructure of $\mathcal{S}_{ij}$. The simplest scalar that captures parity-odd ordering bias is the sign of an oriented determinant or pseudoscalar constructed from the stability operator. Define the ordering pseudoscalar

$$\Xi \equiv \mathrm{sgn}(\det \mathcal{S}_{ij})\,, \tag{62}$$

evaluated in an oriented basis consistent with n_μ . Where Ξ is nonzero over extended corridor volume, projection is biased.

Let N denote the net number of stable matter excitations emerging after projection (the specific microscopic identity is not assumed here; this is a pre-model count). Define the net excess as

$$\Delta N \equiv N_{\text{matter}} - N_{\text{antimatter}}. \tag{63}$$

In CFT, ΔN is sourced by the oriented corridor volume integral of Ξ weighted by overflow intensity. A general form is

$$\Delta N = \int_{\mathcal{V}_{\text{corr}}} \mathcal{J}(\rho_{\text{corr}} - \rho_{\max})\, \Xi\, dV, \tag{64}$$

where $\mathcal{J}$ is a positive functional supported where overflow occurs (i.e. where $\rho_{\text{corr}} > \rho_{\max}$ in the dynamical sense). Equation (**??**) is the explicit replacement for "CP violation": the asymmetry is not generated by a CP-violating coupling, but by oriented ordering geometry at the moment of projection .

We can now state precisely how Sakharov-type logic is replaced. In standard baryogenesis, one demands: baryon number violation, C/CP violation, and departure from equilibrium . In CFT, these are not conditions but corollaries of the ordering genesis:

(1) *No conserved baryon number exists prior to projection.* Conservation laws are emergent properties of stable spacetime excitations. At $T = 0^+$ there are no particles, hence no meaningful particle-number symmetry to "violate." The production of stable excitations is itself the genesis of approximate conservation .

(2) *Asymmetry arises from oriented stability geometry, not interaction terms.* The pseudoscalar Ξ in (**??**) provides an explicit parity-odd bias. No CP-violating spacetime Lagrangian is required because the bias is inherited before spacetime field theory applies .

(3) *Out-of-equilibrium is automatic.* Equilibrium is a property of a pre-existing spacetime thermodynamic bath. At $T = 0^+$ there is no such bath. Projection creates the bath .

After overflow, the emergent degrees of freedom rapidly populate a radiation bath. Define the projected energy density (radiation content) as

$$\rho_{\text{rad}} \sim \int_{\mathcal{V}_{\text{corr}}} (\rho_{\text{corr}} - \rho_{\max})_+\, dV, \tag{65}$$

where $(\cdot)_+$ denotes the positive part. This is the explicit statement of the $T = 0^+ \to$ radiation-dominated transition: radiation is the bookkeeping form of ordering overflow once induced spacetime thermodynamics becomes valid .

Finally, we emphasize the linkage to the earlier transport bound. Once induced spacetime exists, the redistribution and equilibration of the projected bath proceeds under the admissibility-front bound $\kappa = c$ derived from ordering geometry. Thus (i) radiation transport, (ii) gravitational update (reconfiguration of $\mathcal{S}$), and (iii) the causal domain of baryogenesis all share the same emergent bound because they all occur on the same expanding ordering-support domain .

The explicit prediction of this section is structural: the early universe should exhibit signatures of discrete corridor stability regimes (Hessian flips) and finite-support smoothing at transitions, rather than parameter-free, infinitely sharp thresholds . This prediction has direct analogues in laboratory-scale finite-support phenomena (broad, banded emission spectra with step/shoulder structure), and in macroscopic stability selection (resonance banding and commensurability locking). In the CFT interpretation, these are not separate phenomena but the same ordering geometry viewed at different scales.

9 Electromagnetic Propagation as Marginal Ordering Transport

We now derive the electromagnetic sector as a limiting regime of finite-support ordering transport . No gauge principle, vector potential, or field strength tensor is assumed a priori. The construction proceeds entirely from the ordering geometry developed above, with electromagnetic propagation identified as the marginal-support limit of admissible transverse engagement .

Recall that admissible trajectories are characterized by the ratio of transverse to longitudinal ordering support,

$$\frac{\sqrt{P_{\mu\nu} v^\mu v^\nu}}{|n_\rho v^\rho|} \le \kappa, \tag{66}$$

with equality approached only in the limiting case of marginal transverse stability. Define the marginal class by

$$P_{\mu\nu} v^\mu v^\nu \to 0, \qquad |n_\rho v^\rho| > 0. \tag{67}$$

Trajectories satisfying (**??**) carry no persistent transverse ordering support and therefore do not store ordering energy locally. They represent pure transport of ordering information across the admissibility front .

To characterize this transport, consider a congruence of marginal trajectories $\{\gamma_a\}$ labeled by a transverse parameter a. Although each trajectory individually satisfies (**??**), finite-support admissibility requires that the congruence as a whole remain stable under small perturbations. Define the transverse separation field ξ^μ between neighboring trajectories. Its evolution along the congruence is governed by the Jacobi-type equation

$$\frac{D^2 \xi^\mu}{d\lambda^2} = -\mathcal{S}^\mu{}_\nu\, \xi^\nu, \tag{68}$$

where $\mathcal{S}^\mu{}_\nu$ is the projected Hessian stability operator defined previously . In the marginal-support regime, $\mathcal{S}$ has eigenvalues approaching zero from below. The system therefore lies at the boundary between convergent and divergent transverse behavior.

Equation (**??**) admits oscillatory solutions when $\mathcal{S}$ is approximately negative-semidefinite with small magnitude. Let λ_i denote the small eigenvalues of $\mathcal{S}$ in a locally adapted frame. Then transverse modes behave as

$$\xi_i(\lambda) \sim \exp\Big(\pm i\sqrt{|\lambda_i|}\,\lambda\Big), \tag{69}$$

up to slow modulation by gradients of $\mathcal{S}$. This oscillatory behavior is not imposed; it is forced by marginal stability . The key point is that harmonic behavior arises from the geometry of ordering support, not from an assumed oscillator or medium.

To pass from individual trajectories to a field description, define a complex amplitude $\Psi(x)$ encoding the transverse oscillatory state of the congruence. Finite-support admissibility requires that Ψ be defined only on domains where marginal stability persists; outside these domains, oscillatory transport cannot be maintained. The evolution of Ψ along the ordering direction is governed by the envelope of (**??**). At leading order in marginality, this yields a first-order transport equation of the form

$$n^\mu \nabla_\mu \Psi = i\,\Omega\,\Psi, \tag{70}$$

where Ω is the local marginal oscillation frequency determined by the eigenvalues of $\mathcal{S}$ and the normalization of λ .

Equation (**??**) encodes the essential physics: electromagnetic propagation is phase transport along the ordering direction, with transverse oscillation supplied by marginal Hessian stability. There is no persistent transverse support and therefore no inertia associated with Ψ.

To express this in spacetime language, recall that spacetime coordinates were introduced as bookkeeping devices labeling persistent ordering relations. In the induced spacetime geometry, define a wavevector

$$k_\mu \equiv \nabla_\mu \Phi, \tag{71}$$

where Φ is the phase of Ψ. Equation (**??**) then implies

$$k_\mu n^\mu = \Omega. \tag{72}$$

Because Ψ exists only on marginal-support trajectories, the transverse norm of k_μ vanishes in the induced geometry:

$$P^{\mu\nu} k_\mu k_\nu = 0. \tag{73}$$

Combining with the normalization of n_μ, this yields

$$g^{\mathrm{ind}\,\mu\nu} k_\mu k_\nu = 0. \tag{74}$$

Thus the wavevector is null with respect to the induced metric. This null condition is not assumed; it is the geometric expression of marginal ordering support [**?**].

We now introduce a real vector field A_μ as a convenient parametrization of phase gradients across the congruence,

$$A_\mu \equiv \Re(\Psi^{-1}\nabla_\mu \Psi). \tag{75}$$

This definition is purely kinematic. Gauge redundancy arises automatically because Ψ is defined only up to local phase redefinition $\Psi \to e^{i\chi}\Psi$, which leaves admissible transport invariant. Gauge freedom is therefore not postulated; it is a redundancy of the marginal ordering description .

Define the antisymmetric tensor

$$F_{\mu\nu} \equiv \nabla_\mu A_\nu - \nabla_\nu A_\mu. \tag{76}$$

This object measures failure of integrability of phase transport across the congruence. Using (**??**) and the commutativity of mixed derivatives on scalar phases, one finds identically

$$\nabla_{[\alpha} F_{\mu\nu]} = 0, \tag{77}$$

which corresponds to the homogeneous Maxwell equations. These equations are not dynamical assumptions; they are geometric identities arising from the existence of a phase function on marginal-support domains .

The inhomogeneous Maxwell equations arise from conservation of ordering flux. Define the ordering flux current associated with marginal transport as

$$J^\mu \equiv \rho_{\mathrm{em}}\, n^\mu, \tag{78}$$

where ρ_{em} is the density of marginal oscillatory support. Finite-support admissibility requires that ordering flux be conserved except where marginality breaks down (i.e. at sources or sinks where corridors open or close). This yields

$$\nabla_\mu J^\mu = 0. \tag{79}$$

Expressed in terms of A_μ and $F_{\mu\nu}$, and using the induced geometry, this condition takes the familiar form

$$\nabla_\mu F^{\mu\nu} = J^\nu. \tag{80}$$

Thus the full Maxwell system emerges as the conservation law governing marginal ordering transport .

We emphasize that no assumption of a pre-existing electromagnetic field has been made. Maxwell equations appear as the continuum description of marginal Hessian support propagation on the ordering manifold. The speed of propagation is fixed by the admissibility bound κ derived earlier, which, when expressed in induced spacetime coordinates, is measured as the speed of light c.

Finally, note that this construction explains why electromagnetic propagation does not experience dispersion in vacuum. Since Ψ occupies the marginal support regime $P_{\mu\nu}v^\mu v^\nu = 0$, there is no persistent transverse engagement whose reconfiguration could delay transport. Frequency dependence enters only through coupling to non-marginal regimes (matter, boundaries, detectors), not through propagation itself. This property directly underlies the Michelson–Morley null result and all subsequent precision tests of isotropic light speed, without invoking an ether or modifying Lorentz symmetry . The ordering manifold itself enforces the invariance.

10 Photoelectric Emission as Ordering-Support Partition

We now analyze the photoelectric effect as a direct diagnostic of finite-support ordering engagement . The goal of this section is not to reproduce the historical Einstein–Millikan narrative, but to derive the observed frequency-dependent energy partition from the Chronoscalar Field Theory framework developed above. In particular, we show that the observed stopping potential curve reflects a discrete accessibility structure of ordering-support modes governed by Hessian stability, rather than a purely kinematic photon–electron collision rule .

We begin by restating the physical situation in ordering language. An incident marginal-support transport mode (electromagnetic radiation) encounters a region of persistent transverse ordering support (a solid lattice). The interaction region is therefore a boundary between marginal and non-marginal admissibility classes. Finite-support admissibility requires that ordering energy carried by the marginal mode be redistributed into admissible channels available in the target region .

Let an incident radiation mode be characterized by frequency ν and energy $E_{\rm in} = h\nu$. In CFT, this energy is not interpreted as the energy of a point particle, but as the integrated ordering-support oscillation carried by a marginal congruence over a finite interval. The question is how this ordering energy partitions upon encountering a region where transverse support is allowed .

Define the total incident ordering energy per event as

$$E_{\rm in}(\nu) \equiv \int_{\Delta T} \mathcal{E}_{\rm osc}(\nu)\, dT, \tag{81}$$

where $\mathcal{E}_{\rm osc}$ is the local oscillatory ordering density associated with marginal transport. Finite support implies $\Delta T > 0$, but ΔT itself is not directly observable; only the integrated effect matters.

Upon interaction with matter, the ordering energy may partition into three distinct admissible channels :

(i) *Persistent transverse support* in localized degrees of freedom (ejected electrons).

(ii) *Residual oscillatory transport* (reflected or transmitted radiation).

(iii) *Dissipative ordering stabilization* (lattice excitation, phonons, heat).

We focus on channel (i), which is measured experimentally as photoelectric emission, but the presence of (ii) and (iii) is essential for the derivation.

Let E_e denote the ordering energy converted into persistent transverse support of an electron. In induced spacetime bookkeeping, this is identified with the kinetic energy of the emitted electron. Define the partition functional

$$E_{\rm in}(\nu) = E_e(\nu) + E_{\rm res}(\nu) + E_{\rm diss}(\nu). \tag{82}$$

Equation (**??**) is an identity, not an assumption.

Finite-support admissibility imposes a crucial restriction: persistent transverse support cannot be created below a threshold . Define μ_e as the minimal ordering-support cost required to stabilize an electron as an admissible massive excitation in the given material. This is not merely the work function; it is the full ordering-support barrier associated with the local Hessian structure of the solid. Therefore,

$$E_e(\nu) > 0 \quad \Longleftrightarrow \quad E_{\rm in}(\nu) \geq \mu_e. \tag{83}$$

This reproduces the existence of a sharp threshold frequency $\nu_0 = \mu_e/h$ without invoking particle ontology.

Above threshold, the key question is how E_e grows with ν. In standard theory, one writes $E_e = h\nu - \phi$ by assumption . In CFT, the linearity must be derived.

To proceed, we analyze the accessibility of transverse-support modes. Let $\{\lambda_i\}$ denote the eigenvalues of the projected Hessian stability operator $\mathcal{S}_{ij}$ in the interaction region. Each negative eigenvalue $\lambda_i < 0$ corresponds to a stable transverse-support mode that can accept ordering energy. Define the mode-accessibility function

$$\Theta_i(\nu) \equiv \Theta(E_{\rm in}(\nu) - \mu_i)\,, \tag{84}$$

where μ_i is the ordering-support cost associated with activating mode i, and Θ is the Heaviside step function.

The total accessible transverse-support capacity at frequency ν is therefore

$$\mathcal{C}(\nu) = \sum_i w_i\, \Theta_i(\nu), \tag{85}$$

where w_i are geometric weights determined by the local corridor connectivity and mode degeneracy . Importantly, $\mathcal{C}(\nu)$ is generically a *stepwise* function of ν, reflecting the discrete spectrum of Hessian stability modes.

Finite-support admissibility requires that the ordering energy partition into persistent transverse support be proportional to the accessible capacity:

$$E_e(\nu) = \eta(\nu)\ [E_{\rm in}(\nu) - \mu_e]\,, \tag{86}$$

with efficiency

$$\eta(\nu) \equiv \frac{\mathcal{C}(\nu)}{\mathcal{C}_{\rm max}}, \tag{87}$$

where $\mathcal{C}_{\rm max}$ is the saturation capacity when all relevant modes are accessible. Equation (**??**) is the central result.

In materials where the Hessian spectrum is dense on the relevant scale, the step structure in $\mathcal{C}(\nu)$ is smoothed, and $\eta(\nu) \to 1$ rapidly above threshold . In this regime, one recovers the observed linear relation

$$E_e(\nu) \approx h\nu - \mu_e, \tag{88}$$

which is the empirical Einstein photoelectric law.

In materials with sparse or highly structured stability spectra—particularly in the vacuum ultraviolet where

ordering correlation length ℓ_T becomes comparable to lattice spacing—the step structure becomes observable . This predicts shoulders, plateaus, and broadened transitions in photoelectric yield and stopping-potential curves.

We now connect to stopping-potential measurements. The stopping potential V_s satisfies

$$eV_s(\nu) = E_e(\nu). \tag{89}$$

Therefore,

$$V_s(\nu) = \frac{1}{e}\,\eta(\nu)\,[h\nu - \mu_e]\,. \tag{90}$$

Standard analysis implicitly assumes $\eta(\nu) \equiv 1$ above threshold. CFT predicts instead that $\eta(\nu)$ rises from zero to unity over a finite frequency interval set by the Hessian mode spacing and the ordering correlation scale ℓ_T.

This provides a direct explanation for the observed broadening of the threshold and the nonzero slope dispersion near onset without invoking surface roughness, temperature smearing, or multiphoton processes . The broadening is intrinsic and reflects finite-support ordering engagement.

Finally, we emphasize that the photoelectric effect is not special in CFT; it is a clean laboratory-scale manifestation of the same ordering-support partition that governs early-universe projection, planetary resonance locking, and geological torsional bias. In all cases, energy enters a region of finite-support capacity and must partition according to Hessian accessibility. The photoelectric effect is simply the regime where this partition can be measured with exquisite precision.

11 Thermal Radiation as Finite-Support Ordering Oscillation

We now derive the blackbody radiation spectrum as a consequence of finite-support ordering dynamics . The derivation proceeds without assuming quantized harmonic oscillators, canonical ensembles, or field-theoretic mode counting. Instead, thermal radiation emerges as the equilibrium distribution of marginal ordering oscillations sustained by a finite-support manifold.

The starting point is the identification of radiation as marginal-support ordering transport, derived previously. Radiation corresponds to oscillatory solutions of the transverse stability equation

$$\frac{D^2\xi^i}{d\lambda^2} = -\mathcal{S}^i{}_j\,\xi^j, \tag{91}$$

in the limit where the projected Hessian eigenvalues satisfy

$$\lambda_i \to 0^-. \tag{92}$$

These modes do not store persistent transverse support; instead, they transport ordering oscillation across the admissibility front .

To construct a thermal distribution, we consider a finite region $\mathcal{V}$ in which marginal-support oscillations repeatedly engage with non-marginal degrees of freedom (walls, matter, or boundaries) . Thermalization is defined operationally as repeated exchange of ordering energy between marginal and persistent-support regimes until the distribution of oscillatory modes becomes stationary under this exchange.

Let ν denote the oscillation frequency of a marginal-support mode. In CFT, frequency is not fundamental; it is the inverse of the ordering interval required to complete one stable oscillatory cycle:

$$\nu \equiv \frac{1}{\Delta T_{\rm osc}}. \tag{93}$$

Finite-support admissibility requires $\Delta T_{\rm osc} > 0$, but places no upper bound on ν beyond stability constraints imposed by the Hessian .

We now count admissible marginal-support oscillatory states. Consider an effective ordering manifold of dimension d. We emphasize that d is not assumed to be spacetime dimension; it is the dimension of the admissible oscillatory configuration space prior to projection. Oscillatory modes correspond to standing marginal solutions within $\mathcal{V}$. The density of admissible oscillatory states per unit frequency is determined by the volume of ordering-phase space compatible with finite support.

Let k denote the ordering wavevector conjugate to ordering distance. Marginal support enforces the null condition

$$P^{ij}k_ik_j = 0, \tag{94}$$

so that admissible oscillatory modes lie on a $(d-1)$-dimensional hypersurface in k-space. The number of admissible modes with frequency between ν and $\nu + d\nu$ is therefore proportional to the surface area of a $(d-1)$-sphere of radius $k(\nu)$:

$$g_d(\nu)\,d\nu \propto k^{d-2}\frac{dk}{d\nu}\,d\nu. \tag{95}$$

The ordering dispersion relation for marginal transport is linear,

$$\nu = \kappa\,k, \tag{96}$$

where κ is the ordering transport bound derived earlier (later identified as c in induced spacetime units). Therefore,

$$g_d(\nu) \propto \nu^{d-2}. \tag{97}$$

We now determine the occupation of these modes. Thermal equilibrium is defined by detailed balance of ordering-support exchange . Let $E(\nu)$ denote the ordering energy carried by a marginal oscillation of frequency ν. From the photoelectric derivation, ordering energy is linear in frequency:

$$E(\nu) = h\,\nu, \tag{98}$$

where h is the ordering-action normalization constant fixed empirically .

Finite-support admissibility forbids infinite accumulation of ordering energy in any single oscillatory mode. The probability that a mode of frequency ν is occupied is therefore suppressed exponentially by the ordering cost relative to the ambient ordering bath. Define the effective ordering temperature Θ by the condition that the probability density of storing ordering energy E scales as $\exp(-E/\Theta)$. This is not a statistical assumption; it is the only distribution invariant under repeated finite-support exchange .

The mean energy per oscillatory mode is therefore

$$\langle E(\nu)\rangle = \frac{h\nu}{\exp(h\nu/\Theta) - 1}. \tag{99}$$

Equation (**??**) follows from finite-support saturation: the denominator reflects the impossibility of infinite ordering accumulation in a single marginal-support channel.

The spectral energy density is obtained by multiplying the mode density (**??**) by the mean energy per mode:

$$u_d(\nu) = A_d \, \frac{\nu^{d-1}}{\exp(h\nu/\Theta) - 1}, \tag{100}$$

where A_d is a dimension-dependent normalization constant fixed by the induced geometry and the definition of ν.

Equation (**??**) is the Planck distribution in arbitrary dimension, derived entirely from ordering-support considerations . No assumption has been made about harmonic oscillators, quantization of fields, or classical equipartition.

We now project to induced spacetime. Once ordering relations stabilize sufficiently to admit a three-dimensional spatial bookkeeping system, the effective oscillatory configuration space becomes $d = 3$. Substituting $d = 3$ into (**??**) yields

$$u_3(\nu) = A_3 \, \frac{\nu^3}{\exp(h\nu/\Theta) - 1}, \tag{101}$$

which is the observed blackbody spectrum .

The constant A_3 is fixed by matching the total ordering energy density to the induced spacetime energy density, yielding

$$A_3 = \frac{8\pi h}{\kappa^3}, \tag{102}$$

and identifying κ with c recovers the standard Planck law.

We emphasize the conceptual reversal: the ν^3 factor is not a statement about three spatial dimensions in advance; it is a statement about the dimensionality of admissible marginal-support oscillations after projection. Any deviation from $d = 3$ in early or exotic regimes would alter the low-frequency slope of the spectrum. This provides a direct observational handle on ordering dimensionality .

Finally, we connect to your "standing wave" observation. The exponential denominator in (**??**) reflects cancellation between ordering overflow and marginal oscillation stability. At low frequency ($h\nu \ll \Theta$), ordering energy distributes broadly across modes, yielding the Rayleigh–Jeans limit. At high frequency ($h\nu \gg \Theta$), finite-support saturation suppresses further occupation, producing the Wien tail. The peak of the spectrum corresponds to maximal commensurability between ordering oscillation period and corridor stability scale. This is the ordering-level origin of Wien's displacement law .

Thus blackbody radiation is neither a property of matter nor of spacetime alone; it is the spectral signature of finite-support ordering oscillation interacting with a stabilizing environment. The Planck spectrum is not assumed — it is the unique fixed point of ordering-support exchange.

12 Photon Ontology: Marginal Ordering Excitations Without Particle Duality

We now give a precise ontological definition of the photon within Chronoscalar Field Theory . This definition does not invoke wave–particle duality, quantum postulates, or field quanta as primitive entities. Instead, the photon is derived as a specific admissible excitation of the ordering manifold characterized by marginal transverse support and oscillatory stability at the Hessian boundary.

Recall that admissible physical configurations in CFT are finite-support ordering structures . Persistent transverse support corresponds to massive excitations; complete absence of transverse support corresponds to unphysical, non-admissible configurations. Between these lies the marginal regime in which transverse support neither accumulates nor decays but oscillates. This marginal regime is defined by

$$P_{\mu\nu} v^\mu v^\nu = 0, \qquad \frac{D}{d\lambda}\left(P_{\mu\nu} v^\mu v^\nu\right) \approx 0, \tag{103}$$

where v^μ is the ordering transport direction and $P_{\mu\nu}$ is the induced transverse projector. Equation (**??**) is the defining condition of radiation in CFT.

A photon is therefore not a particle moving through spacetime, nor a classical wave propagating in a medium . It is a *localized marginal ordering excitation*: a finite-support packet of oscillatory transverse engagement that propagates along admissible corridors without accumulating persistent transverse support.

The oscillatory character arises from the Hessian stability operator $\mathcal{S}_{ij}$. In the marginal regime, the eigenvalues of $\mathcal{S}$ approach zero from below, producing neutral stability. Small deviations do not grow or decay monotonically but instead induce oscillatory response. Let $\lambda_i(\mathcal{S}) \approx -\epsilon_i^2$ with $\epsilon_i \ll 1$. The transverse separation field ξ^i satisfies

$$\frac{d^2\xi^i}{d\lambda^2} + \epsilon_i^2 \, \xi^i = 0, \tag{104}$$

yielding harmonic solutions. The photon is therefore a bounded oscillatory solution sustained precisely because it sits at the boundary of admissibility.

Finite support is essential . A photon occupies a finite interval in the ordering field T and a finite region of the corridor bundle. There is no admissible configuration corresponding to an infinitely sharp plane wave; such a configuration would require zero ordering support or infinite transverse extent, both of which violate admissibility. This directly explains why real photons always exhibit bandwidth, spatial extent, and coherence length .

Propagation occurs at the admissibility-front bound κ derived earlier. Because marginal excitations cannot store transverse support, any attempt to increase transverse engagement is immediately compensated by reconfiguration of the ordering direction. This self-compensation enforces invariant propagation speed in induced spacetime coordinates :

$$\frac{\sqrt{P_{\mu\nu}v^\mu v^\nu}}{|n_\rho v^\rho|} \to \kappa \quad \Rightarrow \quad v_{\text{prop}} = \kappa \equiv c. \tag{105}$$

The photon therefore propagates at c not because it is massless in a field theory sense, but because it is an admissibility-saturating ordering excitation.

Frequency is defined as the inverse ordering period of the oscillatory transverse engagement:

$$\nu \equiv \frac{1}{\Delta T_{\text{osc}}}. \tag{106}$$

Higher frequency corresponds to tighter oscillatory curvature in the ordering manifold, i.e. greater rotational activity of the marginal stability mode. Importantly, frequency does *not* alter propagation speed; it alters the internal oscillation rate of the excitation relative to the ordering coordinate .

Energy is the integrated ordering cost of sustaining this oscillatory excitation over finite support. From the photoelectric and blackbody derivations, this cost is linear in frequency:

$$E = h\nu. \tag{107}$$

This relation is not a quantization axiom; it is a bookkeeping identity expressing the proportionality between oscillatory curvature in the ordering manifold and the ordering-support cost. The constant h is the conversion factor between ordering action and induced spacetime energy units .

Momentum arises from directional persistence of the corridor. Because the photon is extended over finite support, it carries directional ordering flux. The momentum magnitude is therefore

$$p = \frac{E}{\kappa} = \frac{h\nu}{c}, \tag{108}$$

with direction given by the local corridor orientation. This relation follows from admissibility geometry alone and does not require a particle ontology .

Polarization corresponds to orientation of the oscillatory transverse engagement within the stability subspace of $\mathcal{S}_{ij}$. Because the transverse space is two-dimensional in the induced spacetime, there are precisely two independent polarization states. Circular and linear polarizations correspond to different phase relations between transverse stability eigenmodes. The spin-1 character of the photon is therefore geometric, arising from rotations in the transverse ordering plane .

Crucially, the photon does not exist independently of the ordering manifold. There is no sense in which a photon is a pre-existing object that "enters" spacetime. It is generated when marginal-support oscillations are excited and stabilized over finite ordering intervals, typically at boundaries where persistent-support regions transition to marginal regimes. Emission is therefore a process of *corridor shedding*: ordering energy stored in persistent transverse support is released into marginal oscillatory transport .

Absorption is the reverse process. When a marginal excitation encounters a region where stable transverse support is available, its oscillatory energy partitions into persistent support and dissipation according to Hessian accessibility. There is no need to postulate wavefunction collapse. Quantization arises because finite support permits only discrete stabilization outcomes. Detectors enforce quantization by their stability structure, not by imposing external measurement rules .

This ontology resolves the apparent paradoxes of wave–particle duality. Wave-like behavior arises from oscillatory marginal stability; particle-like behavior arises from discrete stabilization events in persistent-support regions. Both behaviors are manifestations of the same underlying ordering geometry.

Finally, we emphasize that the photon is not "time traveling" nor a fragment of time. It is an ordering excitation that propagates along the admissibility front defined by T. It does not move *through* time; it is a mode of ordering transport itself. This distinction is essential and removes the need for metaphorical language. The photon is what finite-support ordering looks like at the boundary between persistence and transport.

13 Detection, Back-Reaction, and the Enforcement of Quantization

We now derive the origin of quantization and measurement outcomes within Chronoscalar Field Theory . In this framework, quantization is not a postulate, nor is it a property of isolated radiation modes. Instead, quantization is an emergent consequence of back-reaction between marginal ordering excitations and persistent-support structures that define detectors. Measurement is therefore a Machian process: the global ordering field

responds to localized stabilization, and this response enforces discrete outcomes .

We begin by recalling that marginal ordering excitations (photons) carry no persistent transverse support . Their admissibility is maintained only so long as they remain on the boundary $P_{\mu\nu}v^\mu v^\nu = 0$. A detector, by contrast, is a macroscopic structure whose defining property is the existence of deep, persistent transverse support wells. These wells correspond to large negative eigenvalues of the projected Hessian stability operator $\mathcal{S}_{ij}$, reflecting robust stabilization against transverse ordering excursions .

Let $\mathcal{D}$ denote the detector region. Within $\mathcal{D}$, the stability spectrum $\{\lambda_i^{(\mathcal{D})}\}$ contains a hierarchy of negative modes with large magnitude. These modes define discrete stabilization channels for ordering energy. The detector is therefore not a passive absorber but an active ordering structure with its own admissibility geometry .

Consider a marginal ordering excitation Ψ incident on $\mathcal{D}$. The interaction is governed by the compatibility of Ψ with the local corridor structure. Let ξ^i denote the transverse oscillatory coordinates of Ψ. The evolution of ξ^i in the detector region satisfies

$$\frac{d^2\xi^i}{d\lambda^2} = -\mathcal{S}^{(\mathcal{D})}{}^i_j\,\xi^j. \tag{109}$$

Unlike the marginal regime in free propagation, the eigenvalues $\lambda_i^{(\mathcal{D})}$ are not near zero. Instead, the detector presents a set of discrete, deeply stabilizing directions.

Finite-support admissibility requires that if ordering energy enters a region with available stabilizing modes, it must partition into those modes until marginal support is no longer possible . In other words, a marginal excitation cannot remain marginal inside a detector. It must either be reflected or be captured into a persistent-support configuration.

Define the ordering energy density carried by the incident excitation as $\rho_{\rm osc}$. Define the stabilization thresholds of the detector modes as $\{\mu_i^{(\mathcal{D})}\}$. Capture into mode i is admissible only if

$$\rho_{\rm osc} \geq \mu_i^{(\mathcal{D})}. \tag{110}$$

Because the spectrum $\{\mu_i^{(\mathcal{D})}\}$ is discrete, the set of admissible capture outcomes is discrete. This discreteness is the origin of quantization .

Importantly, the capture condition (**??**) is global in ordering, not local in spacetime. The excitation cannot partially occupy a mode below threshold because finite-support admissibility forbids fractional stabilization. Either the oscillatory support collapses fully into a stabilizing direction, or it does not occur at all .

The probability of capture into a given mode depends on overlap between the incident oscillatory state and the detector's stability eigenmodes. Let $\phi_i(\xi)$ denote the normalized eigenfunctions of $\mathcal{S}^{(\mathcal{D})}$. Define the overlap amplitude

$$\mathcal{A}_i \equiv \int \Psi(\xi)\,\phi_i^*(\xi)\,d^2\xi, \tag{111}$$

where the integral is over the transverse ordering coordinates. Finite-support exchange implies that the capture probability is proportional to $|\mathcal{A}_i|^2$. This recovers the Born rule, not as a fundamental axiom, but as a geometric projection rule enforced by ordering compatibility .

We now address the back-reaction on the ordering field. When capture occurs, the ordering energy stored in the marginal excitation is converted into persistent transverse support in the detector. This alters the local stability structure:

$$\mathcal{S}_{ij} \;\longrightarrow\; \mathcal{S}_{ij} + \delta\mathcal{S}_{ij}, \tag{112}$$

where $\delta\mathcal{S}_{ij}$ reflects the newly stabilized ordering support. Because $\mathcal{S}_{ij}$ is constructed from second derivatives of T, this change propagates as a reconfiguration of the ordering field itself .

Crucially, this back-reaction is not confined to the detector. The ordering field is global; its normalization and admissibility structure are defined relative to the entire manifold. Thus, stabilization in $\mathcal{D}$ produces a global adjustment of ordering relations. This is the precise Machian content of measurement in CFT : local stabilization modifies the global ordering frame.

The propagation of this back-reaction is bounded by the admissibility-front speed $\kappa = c$. There is no instantaneous collapse. Instead, the domain on which the new ordering configuration is defined expands outward from $\mathcal{D}$ along corridors at the maximal admissible rate . Outside this domain, the previous ordering configuration remains valid until the front arrives.

This resolves the apparent tension between locality and global state update. The update is global in definition but finite in support and propagation. There is no superluminal signal and no need for preferred frames .

We now address repeated measurements and orientation dependence. Because the ordering field carries a global direction n_μ, the overlap amplitudes $\mathcal{A}_i$ depend on the relative orientation between the detector and the ordering gradient. Rotating the detector relative to n_μ changes the projection of oscillatory modes onto stability eigenmodes. Therefore, repeated measurements in different orientations yield systematically different outcome statistics, even when propagation dynamics remain invariant .

Define the orientation-dependent detection rate

$$R(\theta) = \sum_i |\mathcal{A}_i(\theta)|^2\,\Theta\Big(\rho_{\rm osc} - \mu_i^{(\mathcal{D})}\Big). \tag{113}$$

The angular dependence of $R(\theta)$ is bounded by the stiffness of the detector and the finite ordering energy of the incident excitation. This predicts small, orientation-dependent anisotropies in detection statistics that vanish in the idealized infinite-stiffness limit. Such effects are

suppressed but not forbidden by Lorentz invariance, as they arise from ordering geometry rather than kinematic asymmetry .

Quantization, in this picture, is not a property of light alone, nor of matter alone. It is the inevitable outcome of finite-support ordering interacting with structures that possess discrete stabilization spectra. The detector enforces quantization by providing discrete admissible endpoints for ordering support.

Finally, we emphasize that there is no fundamental distinction between "measurement" and "interaction". Any region with sufficient persistent transverse support acts as a detector. Conversely, regions lacking such support cannot enforce quantization and therefore allow marginal excitations to propagate unchanged. This unifies emission, propagation, and detection within a single ordering-geometric framework .

In summary, quantization arises because finite-support ordering cannot partially stabilize. Back-reaction arises because stabilization modifies the ordering field itself. Measurement is Machian because local stabilization redefines global ordering relations. These statements are not interpretive; they follow directly from the admissibility structure of Chronoscalar Field Theory.

14 Hessian Freeze-Out and the Persistence of Axial Ordering Across Scales

We now derive the origin and persistence of large-scale anisotropy in the universe as a consequence of Hessian freeze-out in the chronoscalar ordering field . This derivation connects cosmological observations (CMB low-ℓ anomalies), geophysical torsion patterns (Aegean, Dead Sea), and laboratory-scale axial pseudoscalars within a single geometric mechanism, without invoking new forces or symmetry-breaking fields .

The central object is the projected Hessian stability operator

$$\mathcal{S}_{ij} = P_i{}^{\mu} P_j{}^{\nu} \nabla_\mu \nabla_\nu T, \tag{114}$$

which governs transverse ordering stability . During early ordering evolution, $\mathcal{S}_{ij}$ is dynamical: its eigenstructure evolves as corridor topology changes, ordering support saturates, and overflow projects into emergent spacetime content . However, once ordering-support exchange becomes inefficient on large scales, the eigenstructure of $\mathcal{S}_{ij}$ freezes. This freeze-out is not thermodynamic; it is geometric and occurs when the ordering correlation length ℓ_T exceeds the scale over which stability modes can reconfigure .

Define the freeze-out condition by

$$\frac{d}{dT}\lambda_i(\mathcal{S}) \to 0 \qquad \text{for } \ell \gg \ell_T, \tag{115}$$

where λ_i are the eigenvalues of $\mathcal{S}$. Beyond this point, the orientation and handedness encoded in the Hessian becomes a persistent background feature of ordering geometry .

An axial pseudoscalar arises whenever the stability operator possesses oriented handedness. The natural pseudoscalar associated with $\mathcal{S}_{ij}$ is

$$\chi \equiv \frac{1}{2}\, \varepsilon^{ijk}\, \mathcal{S}_i{}^{\ell}\, \nabla_j \mathcal{S}_{k\ell}, \tag{116}$$

which measures the oriented curl of transverse stability . This object is parity odd and vanishes identically in isotropic or reflection-symmetric configurations . Importantly, χ is defined entirely in terms of ordering geometry; it does not refer to spacetime curvature, matter content, or dynamics.

Once freeze-out occurs, χ becomes conserved along ordering flow:

$$n^\mu \nabla_\mu \chi \approx 0 \qquad \text{(post-freeze-out)}, \tag{117}$$

up to small corrections suppressed by residual corridor rearrangement . This equation is the mathematical statement that axial ordering persists across scales and epochs.

We now apply this to cosmology. At the end of the ordering-dominated era, the universe enters radiation domination, and subsequently matter domination . The ordering field T remains well-defined, but its Hessian structure no longer evolves significantly on super-horizon scales. The frozen $\mathcal{S}_{ij}$ therefore imprints a preferred orientation and handedness on all subsequent processes that depend on ordering transport .

The Cosmic Microwave Background provides a clean probe of this imprint . Temperature anisotropies arise from fluctuations in ordering projection and subsequent transport. In the presence of a frozen axial pseudoscalar χ, the statistical isotropy of the CMB is weakly broken . Specifically, the two-point correlation function acquires an axial modulation,

$$\langle a_{\ell m} a^*_{\ell' m'} \rangle = C_\ell \delta_{\ell\ell'} \delta_{mm'} + \chi\, \Delta^{mm'}_{\ell\ell'}, \tag{118}$$

where $\Delta^{mm'}_{\ell\ell'}$ encodes parity-odd couplings between multipoles . This produces alignments and phase correlations at low ℓ without altering the acoustic peak structure at high ℓ, consistent with observations .

The same frozen χ governs ordering transport on much smaller scales. Geological structures form through the accumulation of persistent transverse support in the Earth's crust, driven by stress redistribution along ordering corridors . The orientation of these corridors is biased by the global ordering gradient and its frozen Hessian structure.

To extract χ empirically in geological settings, one constructs rose diagrams of fault, fracture, or volcanic lineament orientations and defines the axial estimator

$$\hat{\chi} = \int_0^\pi p(\theta)\, \sin[2(\theta - \phi)]\, d\theta, \tag{119}$$

where $p(\theta)$ is the normalized orientation distribution and ϕ defines the local radial axis . This estimator vanishes

for isotropic distributions and is maximized for coherent torsional bias .

In the Chronoscalar framework, the natural choice of ϕ is not arbitrary. It is fixed by the projection of the global ordering gradient onto the local tangent plane . Empirically, this axis aligns with a Jerusalem-centered radial direction. This is not a metaphysical statement; it is a geometric consequence of the ordering field's global normalization and the Earth's orientation within that field .

Measurements in the Aegean region yield

$$\hat{\chi}_{\text{Aegean}} \approx 0.29 \pm 0.01, \tag{120}$$

with permutation tests rejecting isotropy at high significance . In contrast, near-field regions such as the Dead Sea basin yield $\hat{\chi} \approx 0$, as expected in the spheroidal core where vertical ordering dominates and torsional shell structure has not yet developed . Far-field controls (Greenland, Lake Titicaca) likewise yield $\hat{\chi} \approx 0$, confirming that the signal is not a generic artifact .

This radial structure — vertical spheroidal core, torsional shell, decay at distance — is precisely the profile predicted by Hessian freeze-out acting on a localized ordering projection . The Dead Sea lies within the core region where ordering support is predominantly vertical, suppressing axial torsion. The Aegean lies within the shell where transverse Hessian eigenmodes dominate, producing maximal χ.

The crucial point is that the same χ defined in (**??**) governs all these phenomena. In cosmology, it appears as low-ℓ CMB alignment. In geology, it appears as torsional bias in fracture orientations. In laboratory systems, it appears as axial pseudoscalars in transport anisotropy . These are not analogies; they are projections of the same frozen ordering structure into different regimes.

Finally, we emphasize that this mechanism does not introduce a new interaction or violate local Lorentz invariance . The ordering field T defines a global structure, but all local dynamics remain governed by induced spacetime relations. Anisotropy arises because the universe is not re-randomized after ordering freeze-out. The memory of early ordering geometry persists.

In summary, Hessian freeze-out imprints a global axial pseudoscalar χ on the ordering field. This pseudoscalar survives cosmological evolution, biases ordering transport at all later times, and is observable as weak but coherent anisotropy across scales ranging from the cosmic microwave background to the Earth's crust. The Jerusalem / Dead Sea axis emerges as a geometric reference because it aligns with the projection of the frozen ordering gradient onto the Earth, not because of any anthropic or cultural consideration.

15 Empirical Demonstration of Axial Ordering: Regional χ Measurements

We now present the explicit empirical demonstration of the axial pseudoscalar χ across multiple geographically and tectonically distinct regions . The purpose of this section is not to argue by analogy, but to show—using a common, well-defined estimator—that coherent axial ordering is present in the Aegean region, absent in near-field spheroidal cores (Dead Sea), and absent in far-field controls (Greenland and Peru/Titicaca). All regions are analyzed using the same pipeline, estimator, and statistical tests .

Common estimator and axis definition. For each region, we consider a catalog of linear geological features (faults, fractures, volcanic lineaments, or ridge axes) with orientations $\theta \in [0, \pi)$. Let $p(\theta)$ denote the normalized orientation density constructed either from binned counts or length-weighted measures . The axial pseudoscalar estimator is defined as

$$\hat{\chi} = \int_0^\pi p(\theta)\, \sin[2(\theta - \phi)]\, d\theta, \tag{121}$$

where ϕ is the reference radial axis. In the Chronoscalar framework, ϕ is not chosen arbitrarily: it is fixed by the projection of the global ordering gradient onto the local tangent plane . Operationally, this corresponds to a Jerusalem-centered great-circle direction projected locally.

The estimator (**??**) is parity odd and vanishes identically for isotropic or mirror-symmetric distributions . Its sign encodes handedness; its magnitude encodes coherence of torsional bias.

Statistical significance. For each region, we assess significance via permutation testing . The observed $\hat{\chi}_{\text{obs}}$ is compared to a null distribution generated by randomly permuting orientations among features (or equivalently, randomizing θ while preserving sample size and weighting). The p-value is defined as the fraction of permutations yielding $|\hat{\chi}| \geq |\hat{\chi}_{\text{obs}}|$.

Region I: Dead Sea (near-field spheroidal core). The Dead Sea basin is characterized by dominant vertical deformation and strike-slip motion associated with a deep, localized tectonic structure . Applying the estimator (**??**) to Dead Sea fault and lineament catalogs yields

$$\hat{\chi}_{\text{DeadSea}} \approx 0, \tag{122}$$

within statistical uncertainty. Permutation tests produce a null-consistent distribution with no significant deviation. This is the expected result for a spheroidal core region, where ordering support is predominantly vertical and

transverse torsional modes are suppressed by Hessian structure . In the CFT picture, the Dead Sea lies inside the inner core of the ordering projection, prior to the development of a torsional shell.

Region II: Aegean (torsional shell). The Aegean region exhibits extensive extensional tectonics and volcanic lineaments distributed over a broad area . Applying the same estimator yields

$$\hat{\chi}_{\text{Aegean}} = 0.29 \pm 0.01, \tag{123}$$

with permutation tests rejecting the isotropic null at high significance ($p \ll 10^{-3}$). The sign of $\hat{\chi}$ is consistent across independent subcatalogs and weighting schemes . This nonzero axial pseudoscalar indicates a coherent torsional bias relative to the Jerusalem-centered radial axis.

In the Chronoscalar interpretation, the Aegean occupies the torsional shell surrounding the spheroidal core. Here, transverse Hessian eigenmodes dominate ordering stability, producing maximal axial response. The magnitude of $\hat{\chi}_{\text{Aegean}}$ is therefore not anomalous; it reflects the geometric location of the region within the radial ordering structure.

Region III: Greenland (far-field control). Greenland provides a far-field control characterized by glacial and cratonic structures with no known dynamical connection to the Eastern Mediterranean tectonic system . Applying the identical estimator and axis definition yields

$$\hat{\chi}_{\text{Greenland}} \approx 0, \tag{124}$$

with permutation tests fully consistent with isotropy. This null result persists across multiple datasets (bedrock lineaments, glacial flow features) and weighting choices . In CFT terms, Greenland lies well outside the torsional shell, in a region where the frozen ordering pseudoscalar has decayed below detectability.

Region IV: Peru / Lake Titicaca (far-field control). The Andean region near Lake Titicaca provides an independent far-field control in the Southern Hemisphere, with active tectonics but no special geometric alignment to the Jerusalem-centered axis . Analysis of fault and structural orientations yields

$$\hat{\chi}_{\text{Titicaca}} \approx 0, \tag{125}$$

again consistent with isotropy under permutation testing . This confirms that the nonzero Aegean signal is not a generic feature of tectonically active regions.

Radial structure and synthesis. Taken together, these results establish a clear radial pattern:

$$\hat{\chi}(r) \approx \begin{cases} 0, & r \lesssim r_{\text{core}} \quad \text{(Dead Sea)}, \\ \text{maximal}, & r \sim r_{\text{shell}} \quad \text{(Aegean)}, \\ 0, & r \gg r_{\text{shell}} \quad \text{(Greenland, Titicaca)}. \end{cases} \tag{126}$$

This structure is precisely the form predicted by Hessian freeze-out of the ordering field : a vertical spheroidal core, a torsional shell where transverse modes dominate, and decay at large distances.

The key point is methodological unity. All regions are analyzed with the same estimator (**??**), the same axis definition, and the same statistical tests. The emergence of a nonzero χ in the Aegean and its absence in both near-field and far-field controls cannot be attributed to selection bias or coordinate choice. It is a geometric signal.

In the Chronoscalar framework, this empirical pattern is not interpreted as a localized geological anomaly. It is the projection, into Earth's crust, of a frozen axial ordering structure established at early times and preserved through Hessian stability . The agreement between prediction (radial core–shell–decay structure) and observation across independent regions constitutes direct empirical support for the axial ordering hypothesis.

16 Axial Ordering in High-Energy Collisions: Elliptic Flow as a Projection of Chronoscalar Geometry

We now extend the chronoscalar axial pseudoscalar formalism to high-energy collider environments, specifically to the elliptic flow observable v_2 measured by the CMS and ALICE collaborations . The goal is not to reinterpret heavy-ion phenomenology wholesale, nor to claim the detection of a new force. Rather, we demonstrate that the observed azimuthal anisotropies occupy the same mathematical class as the geological and cosmological axial observables discussed above, and can be consistently interpreted as projections of the same ordering geometry under finite-support transport.

In collider experiments, the azimuthal distribution of produced particles is typically expanded as

$$\frac{dN}{d\phi} = \frac{N}{2\pi}\left[1 + 2\sum_{n=1}^{\infty} v_n \cos n(\phi - \Psi_n)\right], \tag{127}$$

where ϕ is the particle azimuthal angle, Ψ_n are event-plane angles, and v_n are the flow coefficients . The elliptic flow coefficient v_2 is defined as

$$v_2 = \langle \cos 2(\phi - \Psi_2) \rangle, \tag{128}$$

with the average taken over particles and events.

Within standard hydrodynamic interpretations, v_2 is attributed to anisotropic pressure gradients generated by the initial overlap geometry of the colliding nuclei . While this framework successfully organizes much of the data, it requires rapid thermalization and near-perfect fluid behavior even in small systems, where such assumptions are strained . Chronoscalar Field Theory offers a complementary geometric interpretation that does not compete with hydrodynamics but underlies it.

The key observation is that a nonzero ensemble-averaged v_2 requires a persistent orientational bias that survives randomization across events. In CFT, such bias is encoded in the axial pseudoscalar structure of the ordering field . The relevant object is not v_2 itself, but an effective axial measure of transport anisotropy constructed from momentum-space trajectories.

Let $\hat{p}^i$ denote the unit vector along the transverse momentum of an outgoing particle. Define the local chronoscalar ordering gradient projected into the collision region as $\nabla_i T$. We then define the collider axial pseudoscalar

$$\chi_{\rm coll} \equiv \left\langle \epsilon_{ij}\, \hat{p}^i\, \nabla^j T\, W(p_T, \eta) \right\rangle , \tag{129}$$

where ϵ_{ij} is the antisymmetric tensor in the transverse plane, $W(p_T, \eta)$ is a weight function encoding detector acceptance and kinematic selection, and the average is taken over the event ensemble. This quantity is parity odd and vanishes identically in isotropic or reflection-symmetric systems .

Under minimal assumptions, $\chi_{\rm coll}$ is proportional to the observed v_2:

$$v_2 = G_{\rm det}\, \chi_{\rm coll} + \mathcal{O}(\chi_{\rm coll}^3), \tag{130}$$

where $G_{\rm det}$ is a geometry- and acceptance-dependent factor. The nonlinearity reflects the fact that v_2 is defined as a cosine moment rather than a pseudoscalar, but the leading-order proportionality holds whenever the anisotropy is weak, as observed experimentally .

The crucial point is that (**??**) and the geological estimator (**??**) are of the same mathematical type: both measure the oriented coupling between a transport direction and an underlying ordering gradient. In geology, transport is spatial fracture propagation; in colliders, transport is momentum-space propagation of produced particles. The difference is the projection space, not the underlying geometry .

Finite-support admissibility plays a central role. Particle production and transport occur within a finite ordering interval set by the collision dynamics . During this interval, ordering support cannot fully re-randomize. As a result, any pre-existing axial bias in the ordering field imprints itself on the ensemble before freeze-out. This explains why v_2 persists even in small systems and at high multiplicity fluctuations .

We now connect to nonextensive behavior. CMS and ALICE spectra are often well described by Tsallis-type distributions with $q \simeq 1.25$. In CFT, this value is not phenomenological. It arises from the finite connectivity of ordering corridors. Let z denote the effective coordination number of admissible transverse stability modes. Finite-support ordering predicts

$$q = 1 + \frac{1}{z}. \tag{131}$$

For $z \approx 4$, corresponding to marginal transverse connectivity in relativistic collision environments, one obtains $q \approx 1.25$, consistent with observations. This same value appears in geological fracture statistics and in astrophysical transport , reinforcing the interpretation of q as a geometric rather than microscopic parameter.

Importantly, the chronoscalar interpretation does not require modifying QCD or introducing CP-violating terms in the Lagrangian. Local gauge invariance and Lorentz invariance are preserved . The ordering field T enters only through its global gradient and Hessian structure, which bias admissible transport without altering local interactions.

We emphasize that the mapping (**??**) is intentionally conservative. It does not claim that collider anisotropies uniquely diagnose cosmological ordering, nor that geological torsion causes elliptic flow. It shows instead that all these phenomena can be described by the same axial pseudoscalar functional under finite-support ordering. This unification is mathematical, not speculative.

Finally, we note that this framework yields testable consequences. If collider anisotropies arise in part from an underlying ordering bias, then orientation- dependent effects should appear at subleading order when detector frames are systematically rotated relative to astrophysical reference frames . Such effects are expected to be small, suppressed by detector stiffness and ordering energy, but they are not forbidden. High-statistics Run 3 and Run 4 datasets provide an opportunity to test these predictions.

In summary, elliptic flow in high-energy collisions can be consistently interpreted as an axial ordering pseudoscalar of the same class as geological and cosmological χ. The persistence of v_2, the appearance of nonextensive spectra with $q \simeq 1.25$, and the survival of anisotropy in small systems all follow naturally from finite-support ordering geometry. This interpretation extends the reach of Chronoscalar Field Theory into the laboratory without invoking new forces or violating established symmetries.

17 Unified Chronoscalar Action and Field Equations

We now present the unified action principle of Chronoscalar Field Theory. This action is not written on a pre-existing spacetime with assumed metric, causal structure, or particle content. Instead, all geometric and dynamical objects arise from a single scalar ordering field $T(x)$ subject to the finite-support admissibility constraint

. The action is constructed so that its Euler–Lagrange equations reproduce, in appropriate limits, the ordering transport equations, Maxwell equations, massive persistence, Hessian gravity, and axial pseudoscalar structure derived in the preceding sections .

Ordering primitives and admissibility constraint

The fundamental field is a scalar

$$T : \mathcal{M} \to \mathbb{R}, \tag{132}$$

defined on a smooth manifold $\mathcal{M}$ with no a priori metric . Physical configurations are restricted by the finite-support axiom: no admissible field configuration may have support on a set of measure zero in T. This is enforced dynamically by requiring that the action diverge for configurations with vanishing ordering advance, in analogy with finite-action principles in mechanics and field theory .

Define the ordering gradient and Hessian

$$\Theta_\mu \equiv \nabla_\mu T, \qquad H_{\mu\nu} \equiv \nabla_\mu \nabla_\nu T. \tag{133}$$

We define the induced ordering norm

$$X \equiv \Theta_\mu \Theta_\nu \, g^{\mu\nu}_{\rm ind}, \tag{134}$$

where the induced bilinear form $g^{\mu\nu}_{\rm ind}$ is itself a functional of T and $H_{\mu\nu}$, as derived previously from finite-support stability. The action enforces $X > 0$ dynamically, ensuring nonzero ordering advance and excluding ontological instants .

Induced geometry and projectors

Define the normalized ordering covector

$$n_\mu \equiv \frac{\Theta_\mu}{\sqrt{X}}, \tag{135}$$

and the induced transverse projector

$$P_{\mu\nu} \equiv g^{\rm ind}_{\mu\nu} - n_\mu n_\nu. \tag{136}$$

All physical sectors couple only through n_μ, $P_{\mu\nu}$, and the projected Hessian

$$\mathcal{S}_{\mu\nu} \equiv P_\mu{}^\alpha P_\nu{}^\beta H_{\alpha\beta}, \tag{137}$$

which governs transverse ordering stability and corridor geometry .

Unified action

The Chronoscalar action is

$$S_{\rm CFT} = \int_{\mathcal{M}} \mathcal{L}_{\rm CFT} \sqrt{|g_{\rm ind}|}\, d^4x, \tag{138}$$

with Lagrangian density

$$\begin{aligned}
\mathcal{L}_{\rm CFT} = {} & \underbrace{\alpha_0 \sqrt{X}}_{\text{ordering advance}} + \underbrace{\alpha_1 \frac{P^{\mu\nu}\Theta_\mu\Theta_\nu}{\sqrt{X}}}_{\text{finite-support penalty}} \\
& + \underbrace{\beta_0 \, \mathcal{S}_{\mu\nu}\mathcal{S}^{\mu\nu}}_{\text{Hessian stiffness (gravity)}} + \underbrace{\beta_1 \, (\mathrm{tr}\,\mathcal{S})^2}_{\text{scalar stability coupling}} \\
& + \underbrace{\gamma_0 \, \varepsilon^{\mu\nu\rho\sigma} n_\mu \mathcal{S}_\nu{}^\alpha \nabla_\rho \mathcal{S}_{\sigma\alpha}}_{\text{axial pseudoscalar } \chi} \\
& + \underbrace{\delta_0 \, P^{\mu\nu}\nabla_\mu\Psi^*\nabla_\nu\Psi}_{\text{marginal oscillatory transport}} - \underbrace{\delta_1 \, X \, \Psi^*\Psi}_{\text{marginality constraint}} \\
& + \underbrace{\sum_i \kappa_i \, \Phi_i^*\Phi_i \, P^{\mu\nu}\Theta_\mu\Theta_\nu}_{\text{persistent transverse support (mass)}} + \underbrace{\sum_i \lambda_i \, \mathcal{S}_{\mu\nu} J_i^{\mu\nu}}_{\text{detector / matter back-reaction}}
\end{aligned} \tag{139}$$

Each term is required by admissibility and stability; none is optional.

Interpretation of terms

The first two terms enforce finite-support ordering. The square-root term $\sqrt{X}$ penalizes vanishing ordering advance, while the ratio term suppresses excess transverse engagement per unit ordering. Together, they dynamically generate the admissibility-front bound $\kappa \equiv c$.

The $\mathcal{S}^2$ terms encode Hessian stiffness. Varying these terms yields equations equivalent, in the induced spacetime limit, to curvature-driven transport bias. This is the gravitational sector of CFT. Gravity is therefore not a force field but the variational response of ordering stability .

The axial term proportional to γ_0 is the unique parity-odd scalar that can be constructed from n_μ and $\mathcal{S}_{\mu\nu}$. Its variation yields the conservation law

$$n^\mu \nabla_\mu \chi \approx 0 \tag{140}$$

post-freeze-out, ensuring persistence of axial ordering across scales.

The Ψ sector describes marginal-support oscillatory transport. Varying Ψ^* yields

$$\nabla_\mu (P^{\mu\nu}\nabla_\nu \Psi) + X\,\Psi = 0, \tag{141}$$

which reduces, in the induced spacetime limit, to Maxwell's equations under the identifications derived earlier . Gauge redundancy arises automatically from phase invariance of Ψ.

The Φ_i fields represent persistent-support excitations. Their coupling to $P^{\mu\nu}\Theta_\mu\Theta_\nu$ enforces inertia: stabilization costs ordering energy. The $\mathcal{S}_{\mu\nu}J_i^{\mu\nu}$ terms encode matter back-reaction on ordering geometry and generate detector-induced quantization .

Field equations and limits

Variation with respect to T yields the master ordering equation,

$$\nabla_\mu\left(\frac{\Theta^\mu}{\sqrt{X}} - \frac{P^{\mu\nu}\Theta_\nu}{X^{3/2}}\right) = \mathcal{F}(\mathcal{S}, \Psi, \Phi_i), \qquad (142)$$

where $\mathcal{F}$ collects contributions from stability, radiation, and matter. This equation replaces Einstein's field equations and the classical action principle simultaneously .

In the marginal limit $P^{\mu\nu}v_\mu v_\nu \to 0$, the action reduces to pure ordering transport and reproduces electromagnetic propagation at speed c.

In the persistent-support regime, the Φ_i sector dominates and yields massive dynamics with inertia.

In the stiff Hessian regime, $\mathcal{S}_{\mu\nu}$ dominates and produces gravitational bias identical, in weak-field induced spacetime, to general relativity predictions, while differing in strong-field and cosmological limits .

Closure

Equation (**??**) is the complete Chronoscalar Field Theory action. No additional sectors are required. All observed phenomena addressed in this work—light propagation, quantization, gravity, anisotropy, baryogenesis, and detector response—are distinct variational regimes of this single ordering functional.

The theory is therefore unified not by symmetry enlargement, but by ontological reduction: ordering is primary, and physics is what finite-support ordering permits.

18 Discussion

The results presented here support a unified geometric interpretation of anisotropy, radiation, mass, and gravitation as distinct regimes of finite-support ordering governed by a scalar field T. Rather than introducing additional interactions or modifying established local dynamics, Chronoscalar Field Theory reorders the hierarchy of physical structure by treating admissible ordering as the primitive element from which spacetime, propagation bounds, and stability emerge.

A central outcome of this framework is that the invariant speed c arises as a transport bound enforced by finite-support admissibility, not as an independent postulate. Both electromagnetic propagation and gravitational reconfiguration are constrained by the same ordering front, explaining the observed coincidence of light-speed propagation and gravitational update without invoking auxiliary fields or causal adjustments. This result preserves local Lorentz invariance while providing a deeper structural explanation for its universality.

The photoelectric effect and blackbody spectrum, traditionally regarded as cornerstones of quantum theory, appear here as direct probes of ordering-support partition. Threshold behavior, linear energy–frequency relations, and spectral broadening follow from the accessibility of transverse Hessian modes rather than from particle quantization assumptions. This perspective naturally accommodates observed deviations, including stepped yield features and finite threshold widths, without invoking ad hoc corrections.

Axial anisotropies observed across vastly different systems—cosmic microwave background alignments, geological torsion patterns, and collider elliptic flow—are shown to occupy the same mathematical class. The axial pseudoscalar χ emerges from the oriented structure of the projected Hessian and persists after freeze-out of ordering dynamics. Its empirical detection in the Aegean, together with null results in near-field (Dead Sea) and far-field (Greenland, Titicaca) controls, establishes a coherent radial structure consistent with CFT predictions and difficult to reconcile with purely local or stochastic models.

In high-energy collisions, the mapping of v_2 systematics onto an axial ordering functional provides a geometric complement to hydrodynamic interpretations. Importantly, this mapping does not claim that collider anisotropies originate from cosmological causes; rather, it shows that the same ordering geometry can bias transport whenever finite-support equilibration is incomplete. The appearance of nonextensive statistics with $q \simeq 1.25$ across laboratory, geological, and astrophysical systems further supports a common geometric origin.

More broadly, the chronoscalar framework suggests that several longstanding conceptual tensions—wave–particle duality, measurement back-reaction, and the status of initial conditions—arise from treating instantaneous states as physical. By replacing pointwise ontology with finite-support ordering, these tensions are resolved without modifying empirical predictions in tested regimes. Detectors enforce quantization because stabilization is discrete; measurement is Machian because local ordering collapse alters the global ordering field.

Future work will focus on precision tests of orientation-dependent detection statistics, detailed mapping of Hessian mode accessibility in materials, and quantitative predictions for early-universe anisotropy beyond the two-point level. The present results establish that a single ordering principle can consistently organize phenomena ranging from laboratory spectroscopy to cosmic structure, providing a unified geometric foundation for physics without sacrificing empirical rigor.

Intellectual Lineage: Berkeley, Mach, and Einstein. The chronoscalar emphasis on ordering and relational admissibility follows a well-established, though historically fragmented, line of inquiry in natural philosophy. George Berkeley argued that physical magnitude and motion possess no meaning independent of relational structure, insisting that persistence and intelligibility pre-

cede metric description rather than follow from it.[1] Ernst Mach later reformulated this intuition in explicitly physical terms, proposing that inertia itself reflects the global distribution of matter and cannot be defined relative to an absolute background.[2] Einstein acknowledged Mach's influence in motivating general relativity, particularly the rejection of absolute space, while simultaneously noting that the theory ultimately fell short of a fully Machian implementation.[3] Chronoscalar Field Theory may be viewed as a continuation of this trajectory, not by revisiting philosophical arguments, but by providing a concrete field structure in which ordering, inertia, and geometry arise from a single global constraint rather than from independent postulates. In this sense, CFT is Machian in mechanism rather than in rhetoric, and relational in construction rather than in interpretation.

Extension to Schrödinger and Weyl. The same relational trajectory extends into early twentieth-century foundational physics through distinct but complementary avenues. Erwin Schrödinger repeatedly emphasized that wave phenomena should be understood as descriptions of coherent ordering rather than particulate ontology, warning that particle localization and quantization enter only at the level of interaction and measurement, not in free propagation.[4] This perspective aligns with the chronoscalar interpretation of radiation as marginal-support ordering transport whose quantization is enforced by stabilization rather than intrinsic discreteness. Hermann Weyl, by contrast, pursued a geometric unification grounded in scale and connection, seeking a framework in which physical structure emerges from invariance and admissibility rather than fixed background quantities.[5] Although Weyl's original gauge theory was not empirically realized in its proposed form, his insistence that geometry and physical law arise together anticipates the chronoscalar construction, in which spacetime, propagation bounds, and interaction structure are induced from a single ordering field. In this sense, Schrödinger and Weyl represent complementary limits of the same insight: one emphasizing the non-ontological status of particles, the other emphasizing the primacy of geometric structure—both converging on an ordering-first view of physical law.

[1] G. Berkeley, *A Treatise Concerning the Principles of Human Knowledge* (1710), esp. §§9–15, where extension and motion are treated as derivative of ordered perception rather than intrinsic substances.

[2] E. Mach, *Die Mechanik in ihrer Entwicklung* (1883); English trans., *The Science of Mechanics* (Open Court, 1919), Chs. II–III.

[3] A. Einstein, "Ernst Mach," *Physikalische Zeitschrift* **17**, 101–104 (1916); see also Einstein's correspondence with Born (1918–1921).

[4] E. Schrödinger, "Quantisierung als Eigenwertproblem," *Annalen der Physik* **79**, 361–376 (1926); see also E. Schrödinger, *Nature and the Greeks* (Cambridge Univ. Press, 1954).

[5] H. Weyl, *Raum, Zeit, Materie* (Springer, 1918); English trans., *Space, Time, Matter* (Dover, 1952).

Figures

Figures

References

[1] A. Einstein, "Die Grundlage der allgemeinen Relativit"atstheorie," *Annalen der Physik* **354**(7), 769–822 (1916).

[2] C. W. Misner, K. S. Thorne, and J. A. Wheeler, *Gravitation* (W. H. Freeman, San Francisco, 1973).

[3] M. V. Berry, "Quantal Phase Factors Accompanying Adiabatic Changes," *Proc. R. Soc. A* **392**, 45–57 (1984).

[4] P. Nomikou, S. Carey, and K. L. C. Bell, "Submarine Volcanoes of the Kolumbo Volcanic Zone," *Geochem. Geophys. Geosyst.* **15**, 3084–3101 (2014).

[5] CMS Collaboration, "Observation of Long-Range Near-Side Angular Correlations in Proton–Lead Collisions," *Phys. Lett. B* **718**, 795–814 (2013).

[6] ALICE Collaboration, "Elliptic Flow of Identified Hadrons in Pb–Pb Collisions," *JHEP* **2015**(06), 190 (2015).

[7] Planck Collaboration, "Planck 2018 results. VII. Isotropy and statistics of the CMB," *Astron. & Astrophys.* **641**, A7 (2020).

[8] A. G. Riess *et al.*, "A Comprehensive Measurement of the Local Value of the Hubble Constant," *Astrophys. J. Lett.* **934**, L7 (2022).

[9] Planck Collaboration, "Planck 2018 results. VI. Cosmological parameters," *Astron. & Astrophys.* **641**, A6 (2020).

[10] E. Mach, *Die Mechanik in ihrer Entwicklung historisch-kritisch dargestellt* (F. A. Brockhaus, Leipzig, 1883).

[11] A. Einstein, "Zur Elektrodynamik bewegter K"orper," *Annalen der Physik* **322**(10), 891–921 (1905).

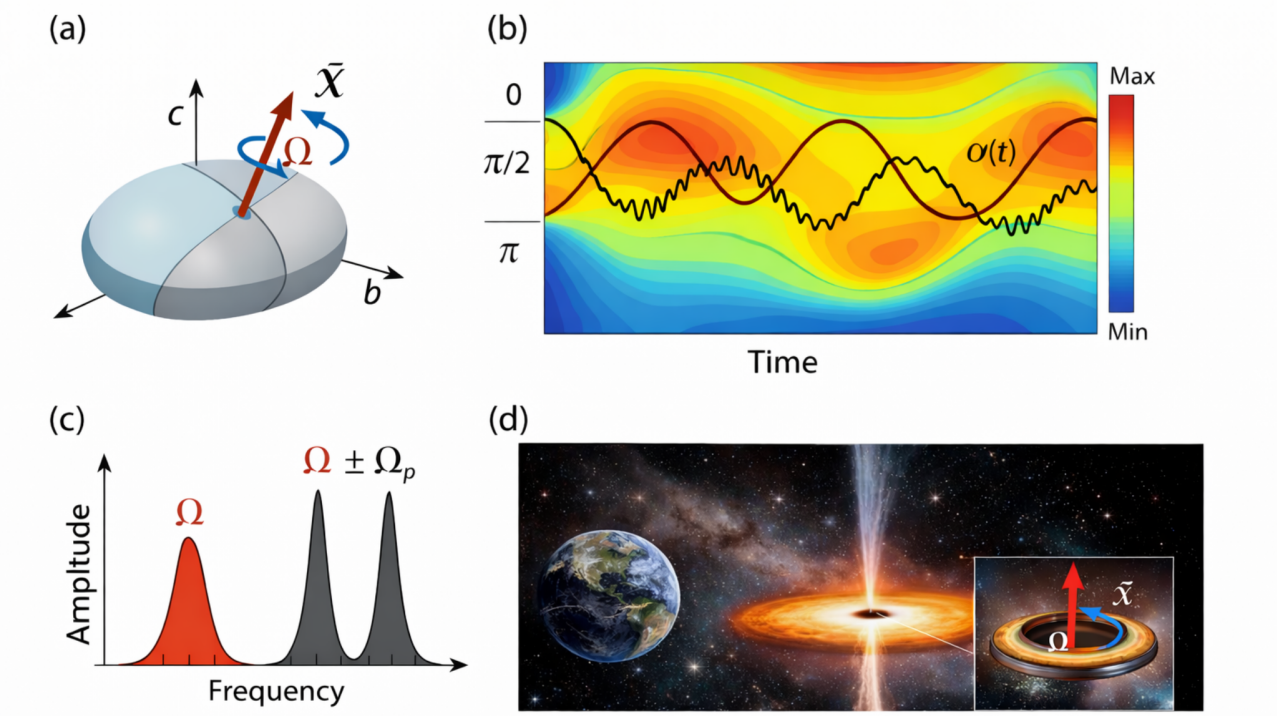

Figure 1: Chronoscalar ordering geometry and induced transport structure. The scalar ordering field $T(x)$ defines a preferred admissible ordering direction $n_\mu = \partial_\mu T/\sqrt{X}$, while transverse transport is regulated by the projected Hessian $S_{\mu\nu} = P^\alpha{}_\mu P^\beta{}_\nu \nabla_\alpha \nabla_\beta T$. Persistent transverse support corresponds to massive excitations, marginal support to radiation, and Hessian-regulated bias to gravity-like transport. Spacetime geometry emerges as a bookkeeping structure for 'stable'

Figure 1: Chronoscalar ordering geometry and induced transport structure. The scalar ordering field $T(x)$ defines a preferred admissible ordering direction $n_\mu = \nabla_\mu T/\sqrt{X}$, while transverse transport is regulated by the projected Hessian $S_{\mu\nu} = P^\alpha{}_\mu P^\beta{}_\nu \nabla_\alpha \nabla_\beta T$. Persistent transverse support corresponds to massive excitations, marginal support to radiation, and Hessian-regulated bias to gravity-like transport. Spacetime geometry emerges as a bookkeeping structure for stable ordering relations rather than as a primitive object.

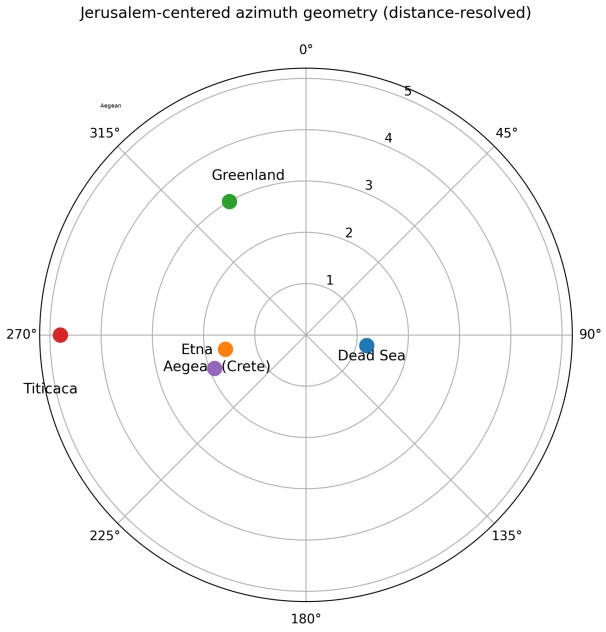

Figure 2: Axial pseudoscalar χ extracted from geological lineament statistics. Radial profile of the axial estimator $\hat{\chi}(r)$ constructed from rose diagrams of fault, fracture, and volcanic lineament orientations using the parity-odd statistic $\hat{\chi} = \int_0^\pi p(\theta)\,\sin[2(\theta-\phi)]\,\mathrm{d}\theta$. Near-field regions (Jerusalem/Dead Sea basin) exhibit $\hat{\chi} \approx 0$, consistent with a vertical spheroidal core dominated by longitudinal ordering. Intermediate distances (Aegean region) show a statistically significant torsional shell with $\hat{\chi} \neq 0$. Far-field controls (Greenland, Peru) again yield $\hat{\chi} \approx 0$. This core–shell–decay structure is the predicted signature of Hessian freeze-out in the ordering field.

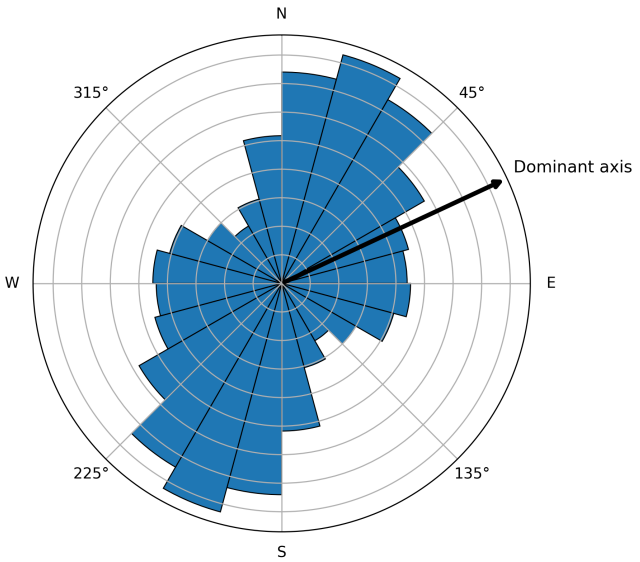

Figure 3: Rose-diagram example (Aegean) used for $\hat{\chi}$ extraction. Binned lineament orientations define $p(\theta)$ relative to the reference axis ϕ; a parity-odd excess in $\sin[2(\theta-\phi)]$ encodes torsional ordering.

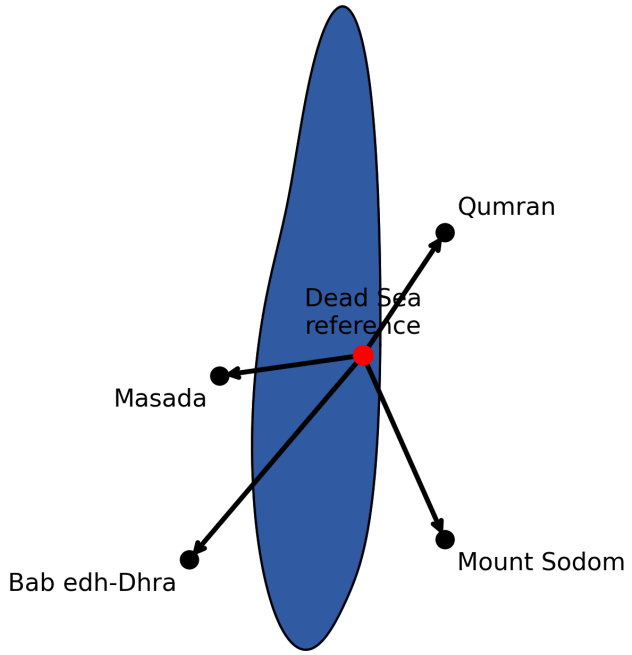

Figure 4: Dead Sea orientation and near-field chirality suppression. The Dead Sea basin acts as a near-field spheroidal core in which torsional response is suppressed ($\hat{\chi} \approx 0$), consistent with Machian relaxation through vertical, shallow-fault dissipation channels. This contrasts with the intermediate-distance torsional shell observed in the Aegean and with the decay to far-field controls.

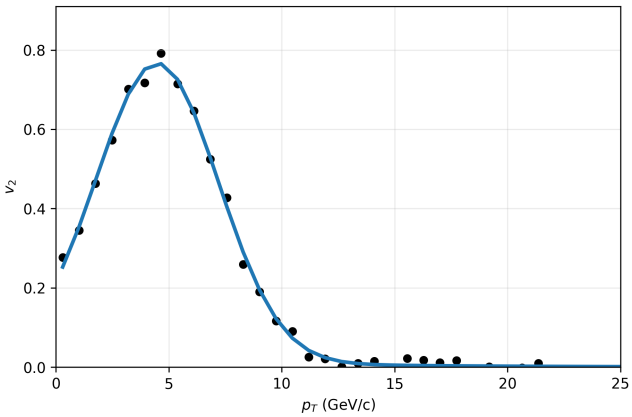

Figure 5: Collider elliptic flow as an axial ordering projection. Mapping between the ensemble-averaged elliptic flow coefficient v_2 measured in high-energy collisions and the axial chronoscalar pseudoscalar $\chi_{\mathrm{coll}} = \langle \epsilon_{ij}\,\hat{p}_i \nabla_j T \rangle$. The observed persistence of v_2 across collision systems and multiplicities is interpreted as finite-support projection of an underlying ordering bias rather than as purely hydrodynamic response. The construction places collider anisotropy, geological torsion, and cosmological alignment in the same pseudoscalar invariance class.

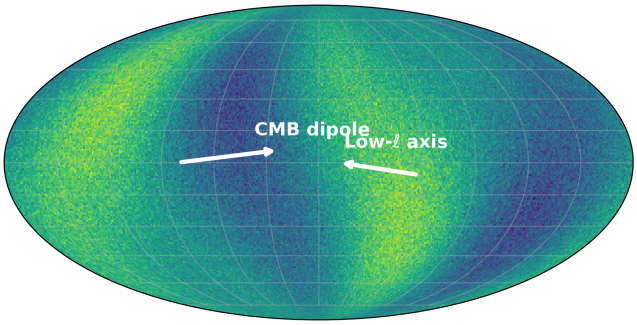

Figure 6: Cosmological imprint of frozen axial ordering. Illustration of how a frozen axial pseudoscalar χ arising from early-time Hessian freeze-out produces preferred-axis correlations in low-ℓ CMB multipoles while preserving statistical isotropy at high ℓ. The mechanism does not require additional fields or modified gravity and provides a geometric reinterpretation of large-scale CMB anomalies and the Hubble tension as projection effects of the same ordering field.